# Very long-term stability of passive margin escarpment constrained by 40 Ar-39 Ar dating of K-Mn oxides

Anicet Beauvais, Nicolas J. Bonnet, Dominique Chardon, Nicolas Olivier Arnaud, Mudlappa J Jayananda

# Very long-term stability of passive margin escarpment constrained by $^{40}Ar$-$^{39}Ar$ dating of K-Mn oxides

Anicet Beauvais [1*], Nicolas J. Bonnet [1], Dominique Chardon [2, 3, 4], Nicolas Arnaud [5], Mudlappa Jayananda [6]

[1] Aix-Marseille Université (AMU), IRD, CNRS, CEREGE UM34, BP 80, 13545 Aix-en-Provence, Cedex 4, France

[2] IRD, UR 234, GET, 14 Avenue Edouard Belin, 31400 Toulouse, France

[3] Université de Toulouse, UPS (OMP), 31400 Toulouse, France

[4] CNRS, GET, 31400 Toulouse, France

[5] Université de Montpellier 2, Géosciences Montpellier, UMR CNRS 5243, 34095 Montpellier, France

[6] Centre for Earth and Space Sciences, University of Hyderabad, P.O Central University Gachibowli, Hyderabad 500 046, India

*Corresponding author: Anicet Beauvais (beauvais@cerege.fr)

Submitted to **Geology**, August 27th, 2015

## ABSTRACT

The post-rift denudation history of high-elevation divergent continental margins is central to decipher "source-to-sink" systems across such margins and to unravel the topographic evolution of their escarpment. We perform $^{40}Ar$-$^{39}Ar$ dating of supergene cryptomelane (K-Mn oxide) from supergene manganese ore deposits to constrain the age of in-situ formed laterites of the low-relief lowland and highland separated by the Western Ghats Escarpment (WGE) of Peninsular India. Documentation of laterites as old as 53 Ma on the highland and 47 Ma at the foot of the WGE shows that the escarpment stabilized before 47 Ma (possibly 60 Ma ago). The geomorphic setting of the dated weathering mantles further allows constraining post-Early Eocene denudation of the lowland and the highland to maximums of 5 and 15 m/My, respectively. These results allow refining apatite fission track thermochronology and cosmogenic radionuclides studies that overestimate 4 to 20 times denudation rates, particularly after escarpment stabilization.


## INTRODUCTION

Constraining the denudation history of high elevation (i.e., escarpment bearing) divergent continental margins documents their post-rift topographic evolution that has implications to quantify their vertical motion, drainage pattern and sedimentary supply over geological time scales. Current evolution models of high-elevation passive margin topography predict contrasted denudation histories. Models based on apatite fission track thermochronology (AFTT) predict a short period (≤ 10-15 Ma) of high denudation focused on a coastal strip resulting in escarpment formation shortly after the onset of rifting (Brown et al., 2002; Braun and van der Beek, 2004; see also Matmon et al., 2002). An alternative model integrating AFTT, the elevation of paleosurfaces and indirect geological constraints argues for successive burials, uplifts and topographic rejuvenations after continental break-up implying that escarpments result from the last uplift episode (Japsen et al., 2012). However, possible thermal instabilities in the shallow crust (< 2 km, i.e., T°< 60°C) and the failure of AFTT models to quantify erosion of crustal sections < 1 km (Brown and Summerfield, 1997) result in large uncertainties in the timing and magnitude of denudation predicted by these models (see also Kohn et al., 2005). Whether and how escarpments are rejuvenated after their formation (e.g., Moore and Blenkinsop, 2006) is also debated because the mode and velocity of their retreat have crucial implications on the evolution of the drainage networks of continental margins and their sedimentary budgets (e.g., Tucker and Slingerland, 1994). Studies based on cosmogenic radionuclides (CRN) predict slow denudation and retreat of escarpments, i.e., 3 to 16 m/My (Bierman and Caffee, 2001), but are only valid over millennial time scales.

Once slow denudation regimes (< 20 m/My) install on continental margins, remnant landscapes may be commonly preserved as a result of limited to moderate relief inversion (Beauvais and Chardon, 2013). In the tropical belt, such paleolandscape remnants are mantled by laterites that may host K-Mn oxydes (cryptomelane) datable by $^{40}Ar/^{39}Ar$ geochronology that already proved beneficial (e.g., Vasconcelos, 1999; Vasconcelos and Conroy, 2003; Beauvais et al., 2008). If properly mapped and dated, lateritic paleolandscape remnants are very useful to calibrate erosion over geological time scales (Beauvais and Chardon, 2013). Here we combine geomorphology with the dating of cryptomelane from in-situ formed lateritic Mn ore deposits preserved at the foot and above the Western Ghats Escarpment (WGE) of Peninsular India as a test of post break-up denudation scenarios deduced from AFTT and CRN studies (Gunnell et al., 2003; Mandal et al., 2015). Our results lead to very low denudation rates (< 5-15 m/My) since stabilization of the escarpment at least 50 Ma ago and argue for a great stability of both the topography and relief of the margin since then.

## GEOMORPHOLOGICAL AND GEOCHRONOLOGICAL OUTLINES

The WGE is up to 1000 m high and was carved into the Deccan traps and their Archean basement (Fig. 1a). The escarpment separates the coastal lowland from the highland plateau and coincides with the continental divide along most of its trace (Fig. 1a). The lowland consists of a weakly dissected lateritic pediment (Figs. 1b and 1c) making the seaward piedmont of the WGE (Widdowson and Gunnell, 1999), on which laterites have been loosely dated to Mid- and Late Tertiary by paleomagnetism (Schmidt et al., 1983). The poorly defined highland laterites would have Late Cretaceous-Eocene paleomagnetic ages (Schmidt et al., 1983). Those laterites are mostly bauxites and mantle a low-relief relict landscape best preserved as 1000-1100 m high mesas near the WGE (e.g., Krishna Rao et al. 1989). Within the highland plateau, relicts of that paleolandscape are sparser (Fig. 1b). At Sandur, $^{40}Ar$-$^{39}Ar$ dating of supergene cryptomelane formed in Mn ore deposits carried by such an highland relict (Figs. 1a and 1b) documents a period of intense lateritic weathering at c. 36-26 Ma (Bonnet et al., 2014), after the formation of Eocene bauxites (Krishna Rao et al., 1989) and before Neogene landscape dissection (Radhakrishna, 1993).

Inversion of apatite fission track data predicts higher denudation in the lowland (up to 120 m/My) than in the highland (< 20 m/My) between 80 and 50 Ma, and low (< 20 m/My) denudation on either side of the escarpment after 40 Ma (Gunnell et al., 2003). This suggests that the WGE formed at c. 50 Ma, after the extrusion of Deccan traps (65 ± 2 Ma) and largely after rifting between India and Madagascar (88 ± 3 Ma).

**FIELD RELATIONSHIPS, MATERIAL AND METHOD**

The lowland pediment consists of a c. 40 km wide concave surface ranging in elevation from 30 to 300 m, and incised by 25 to 100 m deep valleys (Figs. 1b-c). Field observations indicate that the pediment has truncated a bauxitic profile before being in turn weathered and cemented by a ferricrete, which caps a 25 to 60 m thick lateritic weathering profile (Fig. 1c). The studied lowland Caurem and Naveli Mn ore deposits are lentoid pockets within the pediment weathering profiles developed from Archean manganiferous schists and phyllites. The two open cast pits are located at the foot of the WGE at ~ 100 m and 140 m elevation, respectively (Fig. 1c), and four samples were collected at altitudes of 68 m and 45 m in Caurem pit and 113 m and 85 m in Naveli pit (see supplemental material). The highland Sandur Mn ore deposit formed upon Archean manganiferous phyllites and is exposed on a relict lateritic paleosurface capped by a ferricrete at 1012-1015 m elevation (Fig. 1b). Two samples were collected on benches at altitudes of 890 to 975 m (see supplemental material). All samples are massive with botryoidal or cavity filling structures enabling cryptomelane crystallization.

Thorough optical microscopy and X-ray micro-fluorescence analyses of 200-300 μm thin sections allowed separation of eight cryptomelane grains from 300-500 μm symmetrical sections slabs using a binocular magnifier (see Bonnet et al., 2014). The separated grains were characterized using X-ray diffraction, electron microprobe analyses and scanning electron microscopy before irradiation. Cryptomelane ($K_xMn^{IV}_{8-x}Mn^{III}_xO_{16}$) crystallizes into a monoclinic prismatic system with a typical tunnel-type crystal lattice framed by a double chain of $MnO_6$ octahedra and $K^+$ cations in the large tunnel to insure the electronic neutrality of the lattice (Turner and Buseck, 1979). High retentiveness of potassium (content up to 5.5 wt.% K) and radiogenic argon ($^{40}Ar^*$) in the intra-crystalline tunnels warranties the suitability of cryptomelane for $^{40}Ar$-$^{39}Ar$ dating (see Vasconcelos, 1999).

Gas was extracted from the irradiated cryptomelane grains either from a step-wise heating procedure in a double staudacher-type furnace, or from step incremental heating of the grains with a $CO_2$ laser probe power. The gas fractions were then cleaned and analyzed using a VG3600 or Argus IV mass spectrometer. The $^{40}Ar/^{39}Ar$ ages are calculated from plateaus encompassing at least three consecutive $^{39}Ar$ release steps comprising up to 50% of total $^{39}Ar_K$ released, and from best-fit inverse isochrones in $^{36}Ar/^{40}Ar$ vs. $^{39}Ar/^{40}Ar$ correlation diagrams (see also supplemental material).

## RESULTS AND INTERPRETATIONS

The $^{39}Ar$ release spectra of irradiated cryptomelane grains are stacked in the Figures 2a and 2b. Each age spectrum allows calculation of a precise age from a plateau encompassing heating steps overlapping at $2\sigma$ confidence level while degassing at least 5% of the total $^{39}Ar$ released from the highly retentive intra-crystalline sites of cryptomelane structure. The calculated plateau ages also agree well with the isochron ages (Table 1; see also data repositories DR1 to DR2 in supplemental material). The $^{40}Ar$-$^{39}Ar$ ages from the highland Sandur deposit document a weathering period from c. 53 to c. 50 Ma (Fig. 2a and 2c). These ages complement those previously obtained in the same deposit from c. 36 to c. 26 Ma by Bonnet et al. (2014), which are also shown in figures 2a and 2c. The old ages (53-50 Ma) in the highland are interpreted to reflect (bauxitic) weathering of the low-relief relict landscape, whereas the 36-26 Ma weathering period (Bonnet et al., 2014) is interpreted as that having led to the geochemical reworking of the bauxites documented by Krishna Rao et al. (1989). Lateritic profiles of the lowland pediment record weathering periods at c. 47-45 Ma, c. 24-19 Ma, and an episode at c. 9 Ma (Fig. 2b and 2c). The 47-45 Ma ages date the early (bauxitic) weathering of the lowland, whereas the ages between 24 and 19 Ma document renewed weathering and formation of the pediment's capping ferricrete, the 9 Ma age reflecting a discrete weathering pulse.

## DISCUSSION

The preservation of in-situ formed laterites as old as 53-50 Ma above and 47-45 Ma below the WGE indicates that the current topographic envelope of the SW Indian margin corresponds to a bauxitic paleosurface dating from the Early Eocene, which already included the WGE with its present amplitude (Fig. 3). The 47-45 Ma old laterites at 55 m depth underneath the lowland pediment belong to a bauxitic profile that did not exceed 120 m in thickness (e.g., Bardossy and Aleva, 1990). Even if the lowland bauxitic profile had been totally eroded (i.e., 120 m of stripping), the maximum denudation rate of the piedmont between early (bauxitic) weathering (47 Ma) and abandonment of the pediment (19 Ma) would be lower than 5 m/My. Given that incision of the pediment does not exceed 100 m, the incision rate of the WGE' piedmont is less than 6 m/My over the last 19 Ma. Anyhow, the remarkable preservation of the pediment surface argues for negligible net denudation of the piedmont's envelope after c. 20 Ma (Fig. 1c).

Different ages recorded at a same depth in the lowland weathering profiles indicate that preserved old lateritic mantles of the escarpment piedmont have undergone several weathering episodes under a slow mechanical denudation regime. Preservation of 47 Ma old bauxitic weathering mantles at least 60 m thick thus attests that the current escarpment established at least 47 Ma ago, and did not retreat since then. Therefore, escarpment formation or retreat driven by Neogene rejuvenation of the lowland (e.g., Radhakrishna, 1993; Widdowson and Gunnell, 1999) is excluded.

Topographic inversion of the low-relief bauxitic paleolandscape throughout the highland plateau rarely attains 450 m (e.g., Figs. 1b and 3). Therefore, the ages (53-50 Ma) obtained on laterites mantling this relict landscape imply a post-Early Eocene incision rate of less that 9 m/My over the last 50 Ma. Given the very low preservation rate of the old paleolandscape (Fig. 3), this incision rate approximates the denudation rate (Beauvais and Chardon, 2013). Renewed weathering of the highland during the Oligocene (i.e., 36-26 Ma; Bonnet et al., 2014) did not result in significant denudation of the Eocene landscape (< 100 m at Sandur and Belgaum for instance; Fig. 1a; Krishna Rao et al., 1989 and our own field observations). Therefore, erosion rates up to 15 m/My may be expected on the highland over the last 26 Ma.

Formation of 47 Ma-old lateritic bauxites at the foot of the WGE would be in agreement with the last denudation pulse predicted at c. 50 Ma in the lowland (Fig. 2c) from AFTT inversion model (Gunnell et al., 2003). But this also suggests that the escarpment is even older as bauxitic profiles form slowly at 3 to 10 m/My in contexts of tectonic quiescence and limited denudation (Boulangé et al., 1997). Therefore, if the lowland bauxitic profile comprising 47 Ma-old laterite was 120 m thick, it would have taken at least 12 My to develop under an escarpment that should have been stabilized at least 60 Ma ago.

Our results imply denudation rates lower than 5 m/My in the lowland for the last 47 Ma, as opposed to 5-20 m/My (between 40 and 0 Ma) and even 20-70 m/My (between 50 and 40 Ma) from the AFTT model (blue curve in Fig. 2c). Even erosion rates of c. $10^{-2}$ to $10^{-1}$ m/ky (10-100 m/My) derived from CRN studies in riverine sediments (Mandal et al., 2015) are also questionable given the remarkable preservation of thick weathering profiles as old as 47 Ma on the WGE' piedmont. Likewise, the preservation of c. 100 m thick highland Eocene lateritic profiles formed upon the latest basaltic flow (63 Ma) of the Deccan traps (Widdowson and Gunnell, 1999) would be unlikely under such erosion rates or those (15-25 m/My) derived from AFTT between 53 and 45 Ma (red curve in Fig. 2c). Furthermore, AFTT fails to precisely measure or detect less than 1 km of denudation, which corresponds to the height of most passive margin escarpments. In other words, our results suggest that AFTT- or CRN derived denudation rates are largely overestimated and not realistic once the escarpment there.

Given the early installation of very slow denudation regimes across high-elevation margins such as that of Peninsular India, we suggest that the combination of radiometric dating ($^{40}Ar/^{39}Ar$ of K-Mn oxides, or $^{4}He/^{3}He$ of Fe-oxides) of lateritic landscape remnants with apatite (U-Th)/He thermochronological models be a powerful tool to refine the denudation history of divergent margins of the tropical belt.

## CONCLUSION

$^{40}Ar$-$^{39}Ar$ geochronology of supergene cryptomelane formed in situ in supergene manganese ore deposits on either side of the Western Ghats escarpment indicate the development and preservation of an Eocene weathering paleolandsurface mantling the escarpment, attesting of its stability since at least 47-50 Ma, and possibly since 60 Ma. The ages obtained also constrain slow denudation rates of the lowland (< 5 m/My) and the highland (< 15 m/My) of the escarpment after its stabilization. Our results allow refining erosion rates estimated from AFTT and show that absolute dating of lateritic paleolandscape markers may accurately constrain post break-up denudation history of passive margins, with important implications on their sediment delivery histories on geological time scales.

**Acknowledgements-** This work was funded by IFCPAR project 5007-1, the IRD (UR 161) and the CNRS (INSU 2011-CT2). The French Ministry of Research granted N.J.B. with a three years PhD scholarship (ED251, AMU, OSU Pytheas). Two referees are thanked for their comments on an earlier version of the manuscript.

## References

Beauvais, A., and Chardon, D., 2013, Modes, tempo, and spatial variability of Cenozoic cratonic denudation: The West African example: Geochem. Geophys. Geosyst., v. 14, p. 1590-1608.

Beauvais, A., Ruffet, G., Hénocque, O., and Colin, F., 2008, Chemical and physical erosion rhythms of the West African Cenozoic morphogenesis: The $^{39}Ar$-$^{40}Ar$ dating of supergene K-Mn oxides: J. Geophys. Res., v. 113, F04007.

Bierman, P. R. and Caffee, M., 2001, Slow rates of rock surface erosion and sediment production across the Namib desert and escarpment, southern Africa: Am. J. Sci., v. 301, p. 326–358.

Bonnet, N.J., Beauvais, A., Arnaud, N., Chardon, D., and Jayananda, M., 2014, First $^{40}Ar/^{39}Ar$ dating of intense Late Palaeogene lateritic weathering in Peninsular India: Earth Planet. Sci. Lett., v. 386, p. 126–137.

Boulangé, B., Ambrosi, J-P., and Nahon, D., 1997, Laterites and bauxites: In Soils & Sediments: Mineralogy and Geochemistry, H. Paquet & N. Clauer, Eds., Springer Berlin, Heidelberg, pp. 49-65.

Braun, J., and van der Beek, P., 2004, Evolution of passive margin escarpments: what can we learn from low-temperature thermochronology?: J. Geophys. Res., v. 109, F04009.

Brown, R.W., Summerfield, M.A., 1997, Some uncertainties in the derivation of rates of denudation from thermochronological data: Earth Surf. Proc. Landf., v. 22, 239-248.

Brown, R.W., Summerfield, M.A., and Gleadow, A.J.W., 2002, Denudational history along a transect across the Drakensberg escarpment of southern Africa derived from apatite fission track thermochronology: J. Geophys. Research, v. 107, B12, 2350.

Campanile, D., Nambiar, C. G., Bishop, P., Widdowson, M., and Brown, R., 2008, Sedimentation record in the Konkan-Kerala basin: implications fro the evolution of the Western Ghats and the Western Indian passive margin: Basin research, v. 20, p. 3-22.

Chaubey, A.K., Gopala Rao, D., Srinivas, K., Ramprasad, T., Ramana, M.V., and Subrahmanyam, V., 2002, Analyses of multichannel seismic reflection, gravity and magnetic data along a regional profile across the central-western continental margin of India: Marine Geol., v. 182, p. 303-323.

Gunnell, Y., Gallagher, K., Carter, A., Widdowson, M., and Hurford, A.J., 2003, Denudation history of the continental margin of western peninsular India since the early Mesozoic - Reconciling apatite fission-track data with geomorphology: Earth Planet. Sci. Lett., v. 215, p. 187-201.

Japsen, P., Chalmers, J.A., Green, P.F., and Bonow, J.W., 2012, Elevated, passive continental margins: Not rift shoulders, but expressions of episodic, post-rift burial and exhumation: Global Planet. Change, v. 90-91, p. 73-86.

Kohn, B.P., Gleadow, A.J.W., Brown, R.W., Gallagher, K., Lorencak, M., and Noble, W.P., 2005, Visualizing thermotectonic and denudation histories using apatite fission track thermochronology: Rev. Miner. Geochem., v. 58, p. 527-565.

Krishna Rao, B., Satish, P.N., and Sethumadhav, M.S., 1989, Syngenetic and epigenetic features and genesis of the bauxite-bearing laterite of Boknur-Navge, Belgaum district, Karnataka: J. Geol. Soc. India, v. 34, p. 46-60.

Lee J-Y, Marti, K., Severinghaus, J.P., Kawamura, K., Yoo, H-S., Lee, J.B., and Kim, J.S., 2006, A redetermination of the isotopic abundances of atmospheric Ar: Geochim. Cosmochim. Acta, v. 70, 4507–4512.

Mandal, S.K., Lupker, M., Burg, J-P., Valla, P.G., Haghipour, N., and Christl M., 2015, Spatial variability of 10Be-derived erosion rates across the southern peninsular India escarpement: A key to landscape evolution across passive margins: Earth Planet. Sci. Letters, v. 425, p. 154-167.

Matmon, A., Bierman, P., and Enzel, Y., 2002, Pattern and tempo of great escarpment erosion: Geology, v. 30, p. 1135-1138.

Radhakrishna, B.P., 1993, Neogene uplift and geomorphic rejunevation of the Indian Peninsula: Curr. Sci., v. 64, no. 11/12, p. 787-793.

Schmidt, P.W., Prasad, V., and Ramam, P.K., 1983, Magnetic ages of some Indian laterites: Palaeogeogr. Palaeoclimatol. Palaeoecol., v. 44, p. 185–202.

Tucker, G. E., and Slingerland, R. L., 1994, Erosional dynamics, flexural isostasy, and long-lived escarpments: A numerical modeling study: J. Geophys. Res. 99, B6, 12229-12243.

Turner, S., and Buseck, P.R., 1979, Manganese Oxide Tunnel Structures and Their Intergrowths: Science, v. 203, p. 456–458.

Vasconcelos, P.M., 1999, K-Ar and $^{40}Ar/^{39}Ar$ geochronology of weathering processes: Annu. Rev. Earth Planet. Sci., v. 27, p. 183-229.

Vasconcelos, P.M., and Conroy, M., 2003, Geochronology of weathering and landscape evolution, Dugald River valley, NW Queensland, Australia: Geochim. Cosmochim. Acta, v. 67, no. 16, p. 2913-2930.

Widdowson, M., and Gunnell, Y., 1999, Tertiary palaeosurfaces and lateritization of the coastal lowlands of western peninsula India: in Palaeoweathering, Palaeosurfaces and Related Continental Deposits, Thiry, M., and Simon-Coinçon, R., Eds., International Association of Sedimentologists, Sp. Pub., v. 27, p. 245-274.

Whiting, B.M., Karner, G.D., and Driscoll, N.W., 1994, Flexural and stratigraphic development of the West Indian continental margin: J. Geophys. Research, v. 99, p. 13791-13811.

## Table caption

**Table 1.** Plateau and isochrone ages obtained for the cryptomelane separated from samples collected in highland Sandur and lowland Caurem (CAU) and Naveli (NAV) Mn ore pits. Depth indicates the sampling level below the surface. MSWD = Mean

square weight deviation of isochron. ($^{40}Ar/^{36}Ar_{atm}$ = 298.56 ± 0.31 from Lee et al., 2006).

## Figures caption

**Figure 1**. **(a)** Topo-bathymetric setting of the Southwestern Indian margin. **(b)** Topographic cross-section from Sandur to the escarpment edge in the highland and Goa in the lowland (section trace on Fig. 1a). **(c)** Synthetic Cross-section of the lowland piedmont passing through the two dated Mn ore pits.

**Figure 2**. Stacked $^{40}Ar$-$^{39}Ar$ age spectra of cryptomelane from **(a)** the highland and **(b)** the lowland Mn ore pits (located on Fig. 1). **(c)** Weathering periods derived from series of $^{40}Ar$-$^{39}Ar$ plateau ages including $\sigma$ errors, with denudation rate curves derived from inversion model of apatite fission track data (Gunnell et al., 2003), both for the highland (HL) and lowland (LL). (The 36-26 Ma ages are from Bonnet et al., 2014).

**Figure 3**. Cross-section of the Southwestern Indian divergent margin from offshore basin (A) to Goa, escarpment edge (B) and Sandur (C) (section trace on Fig. 1a). The offshore section including sedimentary limits is adapted from Chaubey et al. (2002), and proportions of clastics are derived from Campanile et al. (2008). Very low offshore accumulation of clastic sediments and correlative Eocene to Mid-Miocene carbonate production (Whiting et al., 1994; Chaubey et al., 2002; Campanile et al., 2008) agrees with onshore weathering and very slow mechanical denudation in the lowland.

Table 1

| Sample ID | Depth ± 2 m | Plateau age ± 2σ (Ma) | % $^{39}Ar$ released | Isochron age ± 2σ (Ma) | $^{40}Ar/^{39}Ar$ intercept ± 2σ | MSWD |
|---|---|---|---|---|---|---|
| **Highland** | | | | | | |
| KMK-2 | -37 | 49.60 ± 1.34 | 100 | 49.60 ± 1.41 | 302.0 ± 25 | 0.10 |
| KPA-8 | -125 | 53.21 ± 3.43 | 76 | 53.01 ± 3.45 | 296.4 ± 13 | 0.40 |
| **Lowland** | | | | | | |
| NAV-4 | -27 | 20.84 ± 1.68 | 54 | 21.12 ± 0.45 | 288.0 ± 6 | 0.33 |
| CAU-1c | -32 | 21.92 ± 0.23 | 56 | 22.07 ± 0.24 | 294.0 ± 1 | 2.28 |
| CAU-1a | -32 | 23.67 ± 0.29 | 57 | 23.67 ± 0.29 | 294.9 ± 2 | 2.31 |
| NAV-3f | -55 | 8.65 ± 0.16 | 84 | 8.57 ± 0.59 | 308.7 ± 94 | 0.55 |
| CAU-3f | -55 | 19.35 ± 1.52 | 58 | 20.22 ± 0.35 | 283.9 ± 18 | 0.05 |
| CAU-3a | -55 | 23.65 ± 0.21 | 54 | 23.71 ± 0.21 | 295.5 ± 2 | 1.85 |
| NAV-3b | -55 | 45.08 ± 0.78 | 57 | 45.15 ± 0.74 | 293.7 ± 3 | 2.04 |
| NAV-3c | -55 | 47.07 ± 0.54 | 60 | 47.11 ± 0.53 | 293.5 ± 3 | 1.25 |

**TABLE 1**

Figure 1

Click here to download Figure Figure. 1(rev.f).jpg

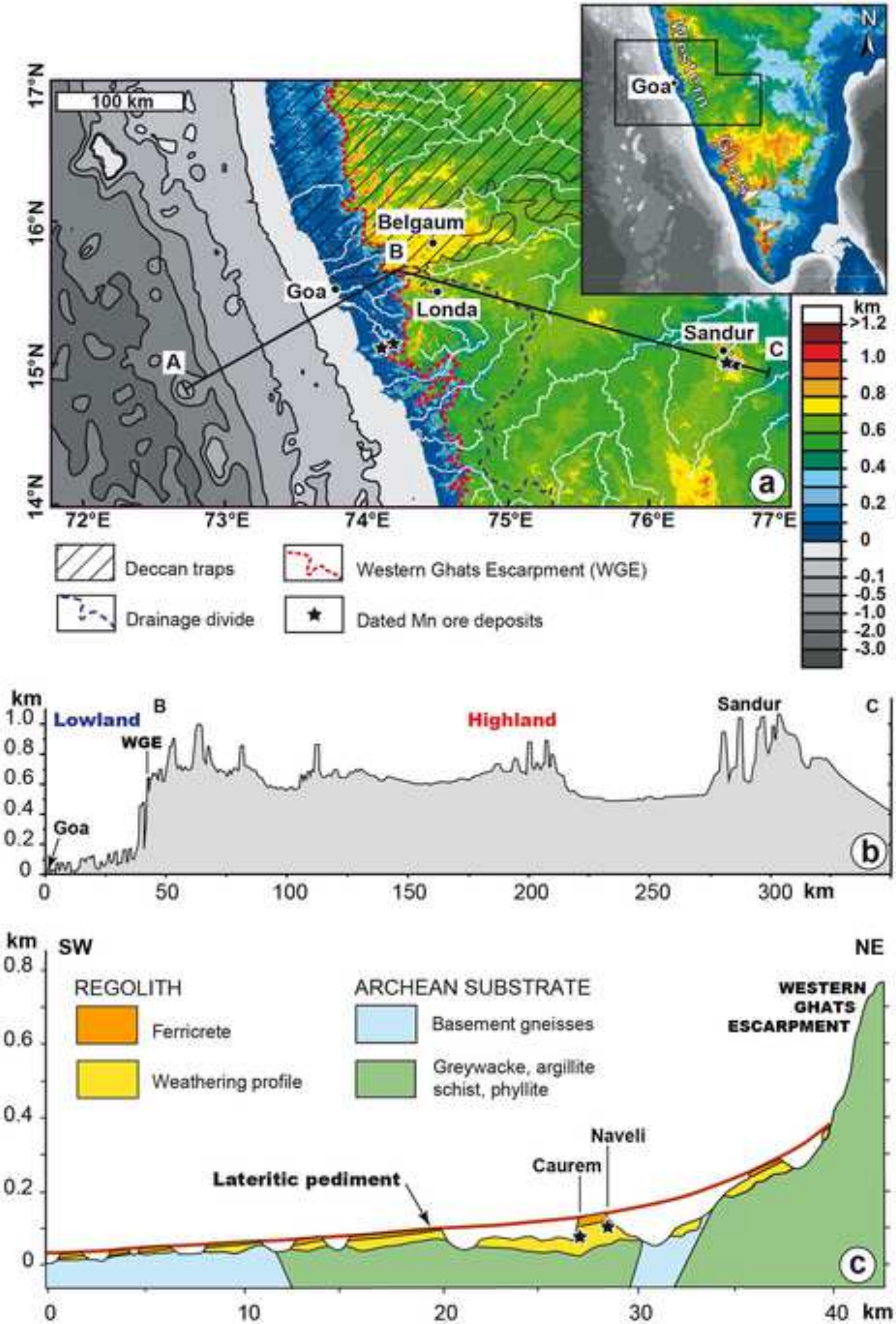


FIGURE 1

 

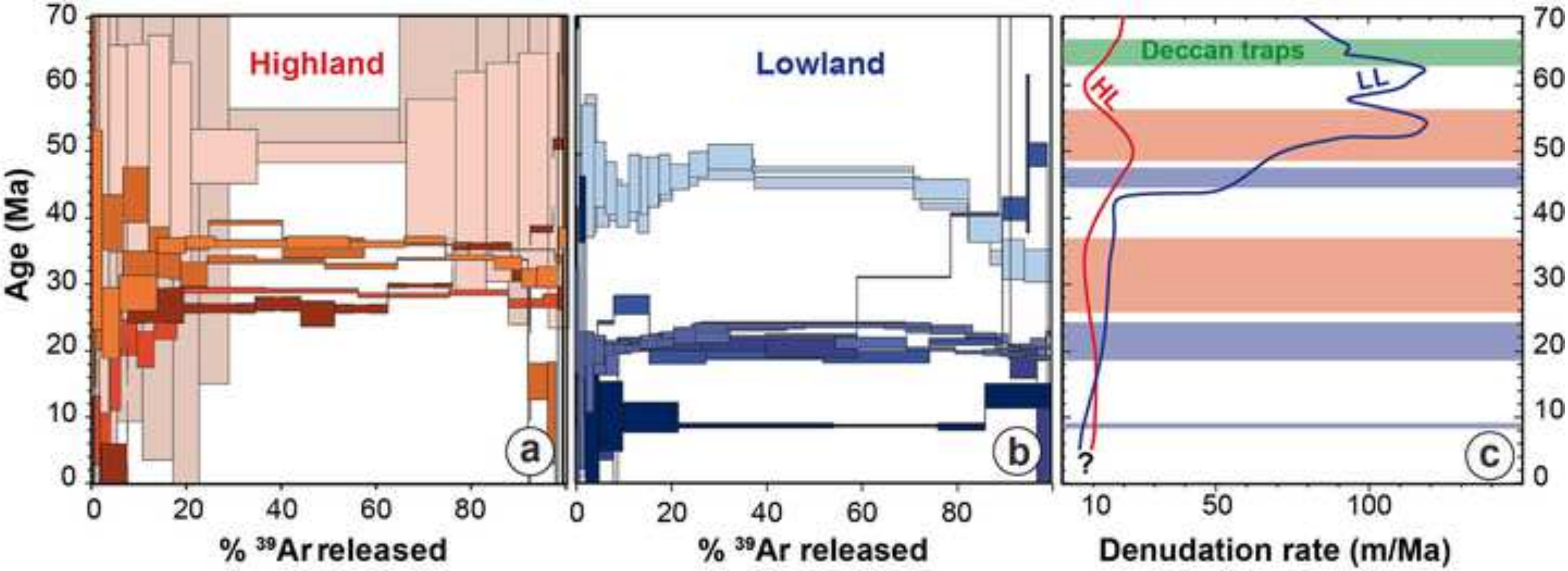
Highland
Lowland
Deccan traps
HL
LL
?
a
b
c
Age (Ma)
% $^{39}$Ar released
% $^{39}$Ar released
Denudation rate (m/Ma)
0
10
20
30
40
50
60
70
0
20
40
60
80
10
50
100

FIGURE. 2

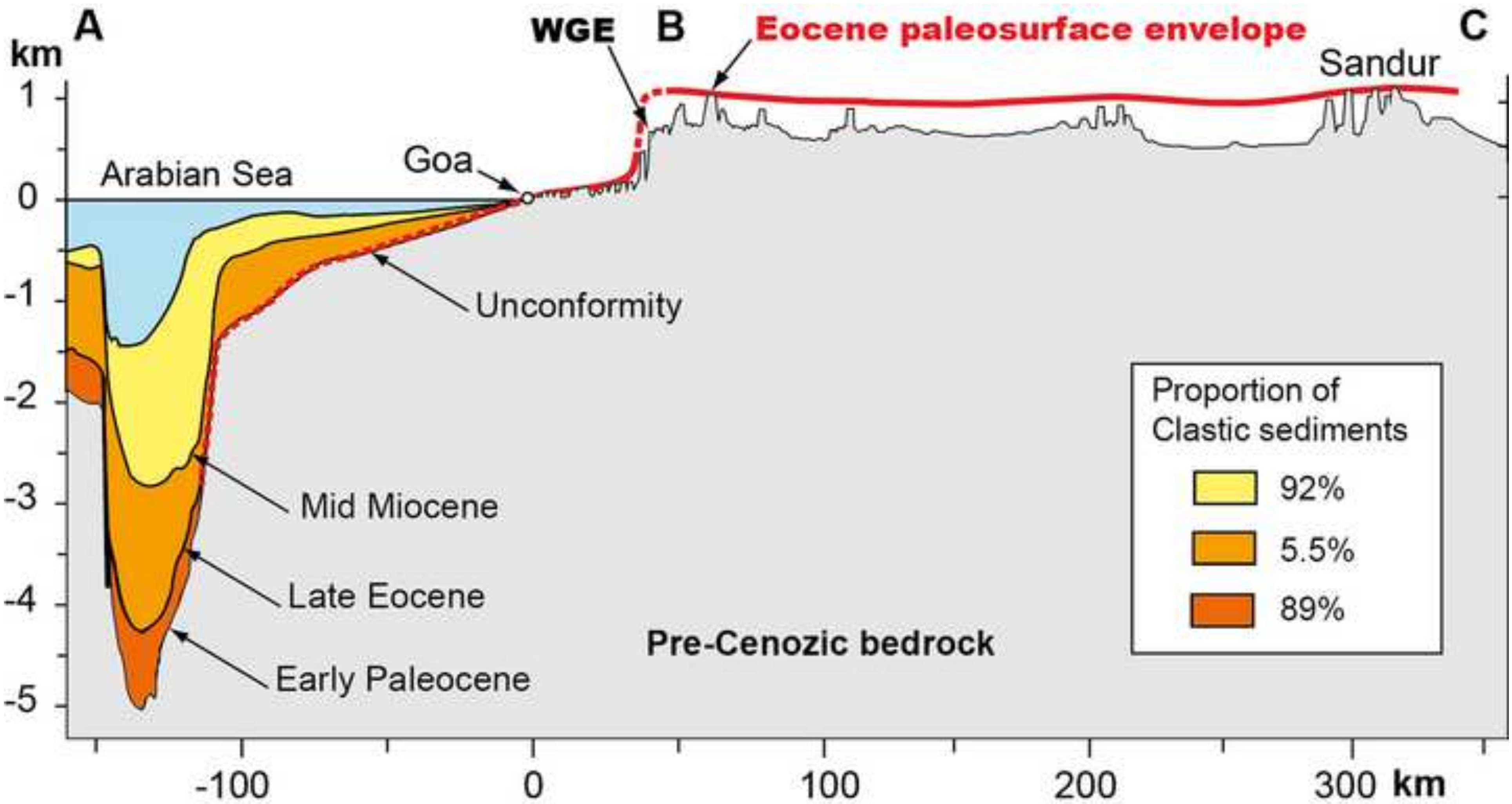
A
WGE
B
Eocene paleosurface envelope
C
km
Sandur
1
Arabian Sea
Goa
0
-1
Unconformity
-2
Proportion of
Clastic sediments
92%
5.5%
89%
-3
Mid Miocene
-4
Late Eocene
Pre-Cenozic bedrock
Early Paleocene
-5
-100
0
100
200
300
km

FIGURE 3

**Beauvais et al., 2015, Very long term stability of passive margin escarpment constrained by $^{40}$Ar-$^{39}$Ar dating of K-Mn oxides**

## Supplementary material

Manganiferous ore samples have been sampled in upland Sandur ore deposits (KPA-8: 15° 0' 2.27"N/76° 32' 41.6"E; KMK-2: 14° 59' 48.34"N/76° 34' 40.34"E) and in lowland ore deposits, Naveli (NAV-3: 15° 07' 55.10"N/74° 09' 49.72’’E; NAV-4: 15° 08' 07.12"N/74° 09' 32.26’’E), and Caurem (CAU-1: 15° 07' 2.19"N/74° 08' 39.66"E; CAU-3: 15° 07' 3.47"N/74° 08' 38.97"E).

Cryptomelane grains were separated from 300-500 μm thick slabs by hand picking. The separated grains were ultrasonically cleaned in absolute ethanol and conditioned in aluminium foil packets, to be irradiated for 50 hours in the TRIGA Mark-II reactor of Pavia University (Italia). The Factor J was determined from the analysis of the standard Taylor Creek Rhyolite sanidine-2 (TCRs-2) monitor, with an age of 28 ± 0.08 Ma (Baksi et al., 1996). The standard was analyzed after every ten unknown samples. After a two-month “cooling” period, the irradiated cryptomelane grains were loaded in a double vacuum Staudacher-type furnace for step heating Ar isotopes measurements. The furnace temperature was calibrated by means of a classical thermocouple, and the gas purification was accomplished using a cold trap with liquid air and Al–Zr AP10 getters (one hot, one cold) for 8 minutes before the introduction into the VG3600 mass spectrometer. One minute was allowed for equilibration before analysis. $^{40}$Ar and $^{39}$Ar were measured on a Faraday cup with a resistor of $10^{11}$ ohm, while $^{39}$Ar, $^{38}$Ar, $^{37}$Ar, and $^{36}$Ar were analyzed using a scintillator and photomultiplier after interaction on a Daly plate. The analytical data are reported in data repositories (Figures DR1 and Table DR2), and the errors are quoted at the 1σ level. Plateau ages are calculated from at least three consecutive $^{39}$Ar release steps comprising up to 50% of total $^{39}Ar_K$ released and overlapping at the 2$\sigma$ confidence level (Fleck et al., 1977). Isochrone ages are accepted when mean square weighted deviation (MSWD) is less than 2.5 and the $^{40}Ar/^{36}Ar$ intercept within 2σ from the $(^{40}Ar/^{36}Ar)_{atm}$ value of 298.56 ± 0.31 (Lee et al., 2006 ; Renne et al., 2009).

## References cited


Baksi, A.K., Archibald, D.A., and Farrar, E., 1996, Intercalibration of $^{40}Ar^{39}Ar$ dating standards: Chem. Geol., v. 129, p. 307-324.

Fleck, R.J., Sutter, J.F., and Elliot, D.H., 1977, Interpretation of discordant $^{40}Ar/^{39}Ar$ age-spectra of mesozoic tholeiites from Antarctica: Geochim. Cosmochim. Acta, v. 41, p. 15-32.

Lee J-Y, Marti, K., Severinghaus, J.P., Kawamura, K., Yoo, H.S., Lee, J.B., and Kim, J.S., 2006, A redetermination of the isotopic abundances of atmospheric Ar: Geochim. Cosmochim. Acta, v. 70, p. 4507–4512.

Renne, P.R., Cassata, W.S., and Morgan, L.E., 2009, The isotopic composition of atmospheric argon and 40Ar/39Ar geochronology: time for a change: Quat. Geochron., v. 4, p. 288-298.


**Figure. DR1**. $^{39}Ar$ releasing spectra showing well defined plateau ages with K/Ca (grey) and Ar* (black) step curves (left) and inverse isochrone diagrams (right) of cryptomelane grains from the open pits samples of **(A)** Sandur **(B)** Naveli and **(C)** Caurem Mn ore deposits (MSWD = mean square weighted deviation).

**Tables. DR2-DR3**. Analytical results obtained for highland and lowland cryptomelane grains, either from Laser energy (spectrometer Argus IV) or double vacuum Staudacher-type furnace temperature, T °C, (spectrometer VG 3600) for each irradiated crypromelane grain. The concentrations of $^{36}Ar$, $^{37}Ar$, $^{38}Ar$, $^{39}Ar$ and $^{40}Ar$ with their respective 1σ error are provided for each step heating. The amount of $^{40}Ar^*$ (%), of $^{39}Ar$ released (%$^{39}Ar$) and the K/Ca ratio (derived from $^{39}Ar/^{37}Ar$) are also given. Finally, this table show ratios $^{40}Ar^*/^{39}Ar_k$ used to determine the corresponding apparent ages, which are presented in the last column with their associated 2σ error. The different J-Factor values are also provided for each irradiated grains.

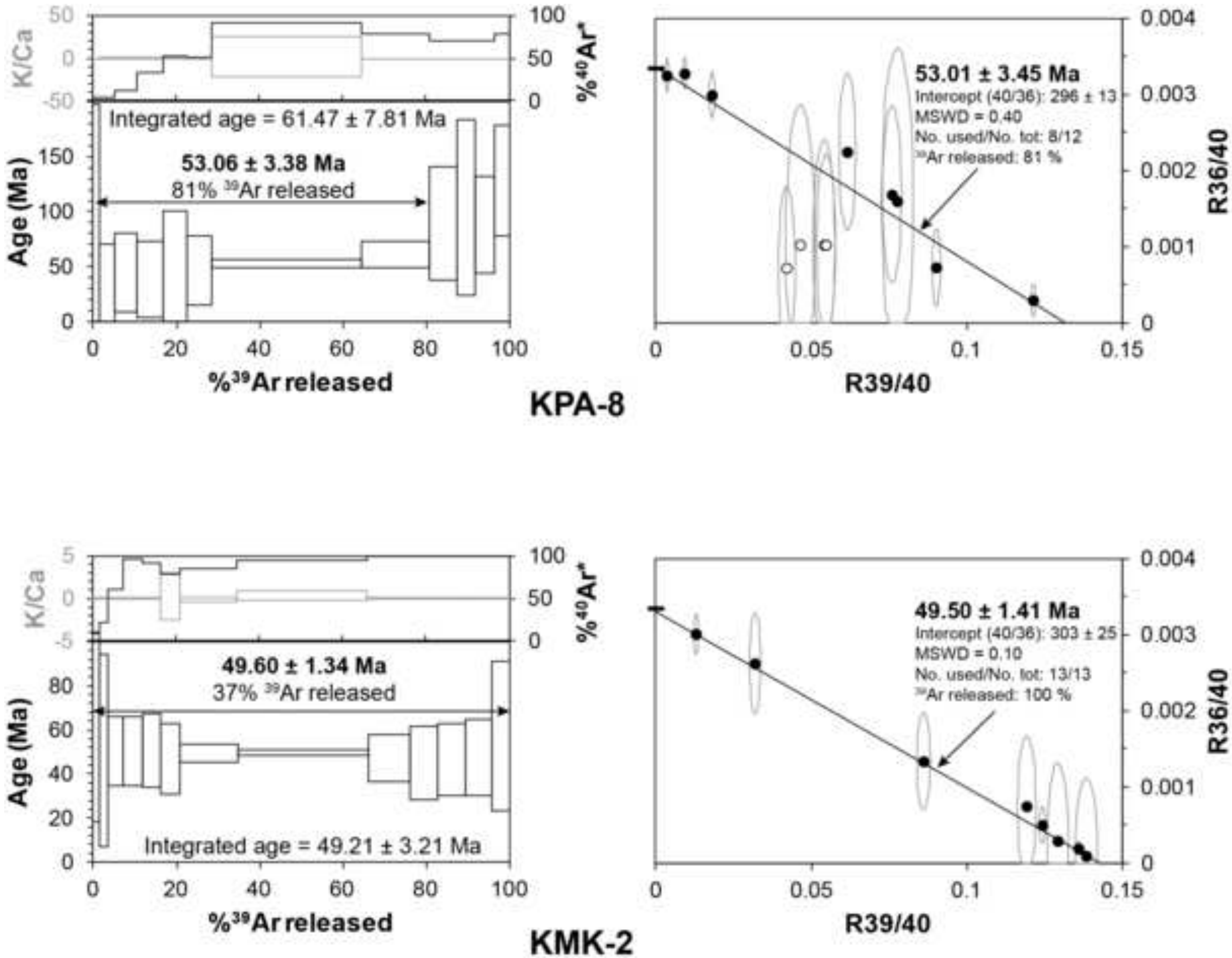
K/Ca
%$^{40}$Ar*
Integrated age = 61.47 ± 7.81 Ma
53.06 ± 3.38 Ma
81% $^{39}$Ar released
Age (Ma)
%$^{39}$Ar released
53.01 ± 3.45 Ma
Intercept (40/36): 296 ± 13
MSWD = 0.40
No. used/No. tot: 8/12
$^{39}$Ar released: 81 %
R36/40
R39/40
KPA-8
49.60 ± 1.34 Ma
37% $^{39}$Ar released
Integrated age = 49.21 ± 3.21 Ma
49.50 ± 1.41 Ma
Intercept (40/36): 303 ± 25
MSWD = 0.10
No. used/No. tot: 13/13
$^{39}$Ar released: 100 %
KMK-2

Figure. DR1- A

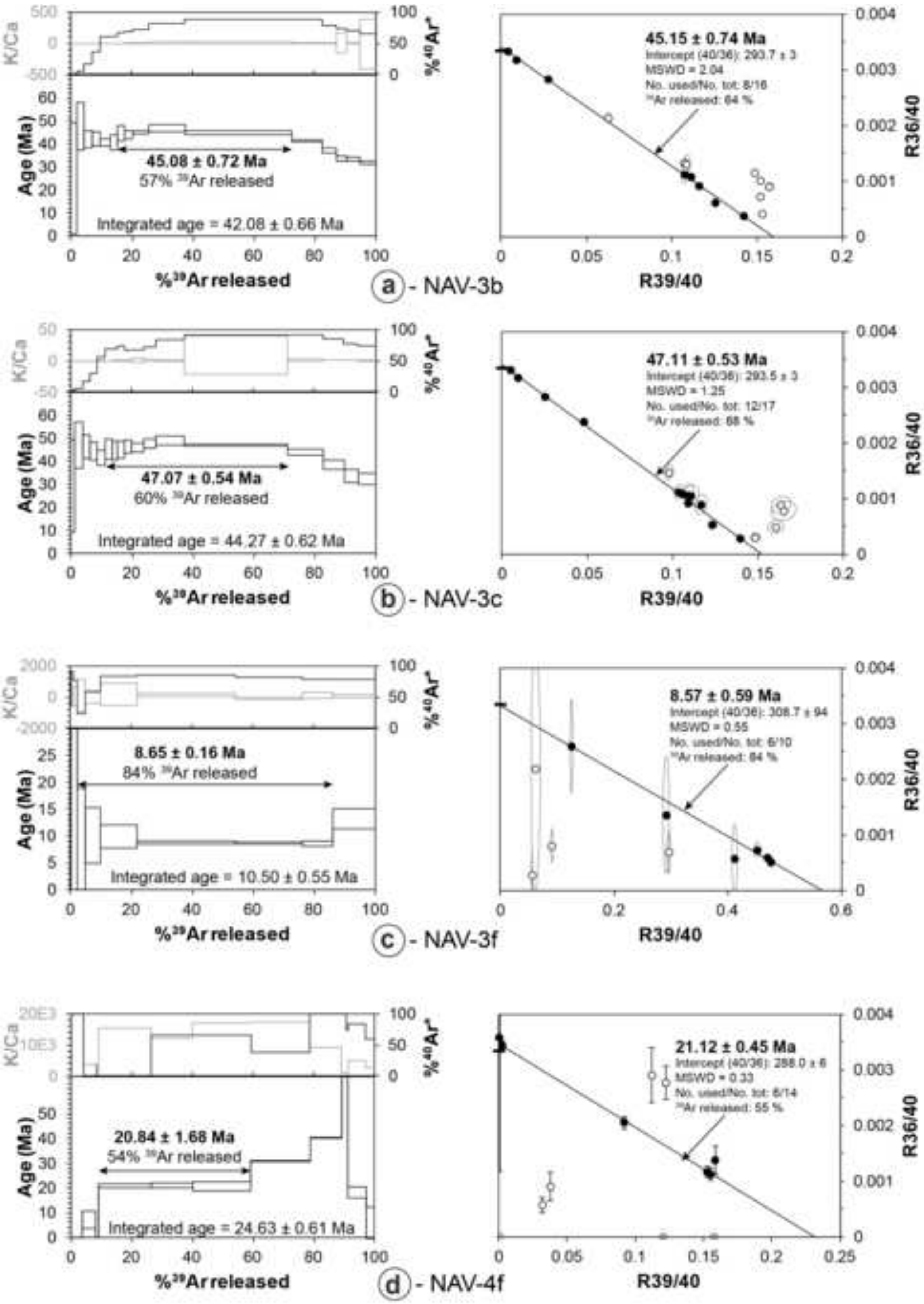
K/Ca
%$^{40}$Ar*
Age (Ma)
45.08 ± 0.72 Ma
57% $^{39}$Ar released
Integrated age = 42.08 ± 0.66 Ma
%$^{39}$Ar released
45.15 ± 0.74 Ma
Intercept (40/36): 293.7 ± 3
MSWD = 2.04
No. used/No. tot: 8/16
$^{39}$Ar released: 64 %
R36/40
R39/40
a - NAV-3b
47.07 ± 0.54 Ma
60% $^{39}$Ar released
Integrated age = 44.27 ± 0.62 Ma
47.11 ± 0.53 Ma
Intercept (40/36): 293.5 ± 3
MSWD = 1.25
No. used/No. tot: 12/17
$^{39}$Ar released: 68 %
b - NAV-3c
8.65 ± 0.16 Ma
84% $^{39}$Ar released
Integrated age = 10.50 ± 0.55 Ma
8.57 ± 0.59 Ma
Intercept (40/36): 308.7 ± 94
MSWD = 0.55
No. used/No. tot: 6/10
$^{39}$Ar released: 84 %
c - NAV-3f
20.84 ± 1.68 Ma
54% $^{39}$Ar released
Integrated age = 24.63 ± 0.61 Ma
21.12 ± 0.45 Ma
Intercept (40/36): 288.0 ± 6
MSWD = 0.33
No. used/No. tot: 6/14
$^{39}$Ar released: 55 %
d - NAV-4f

**FIGURE. DR1-B**

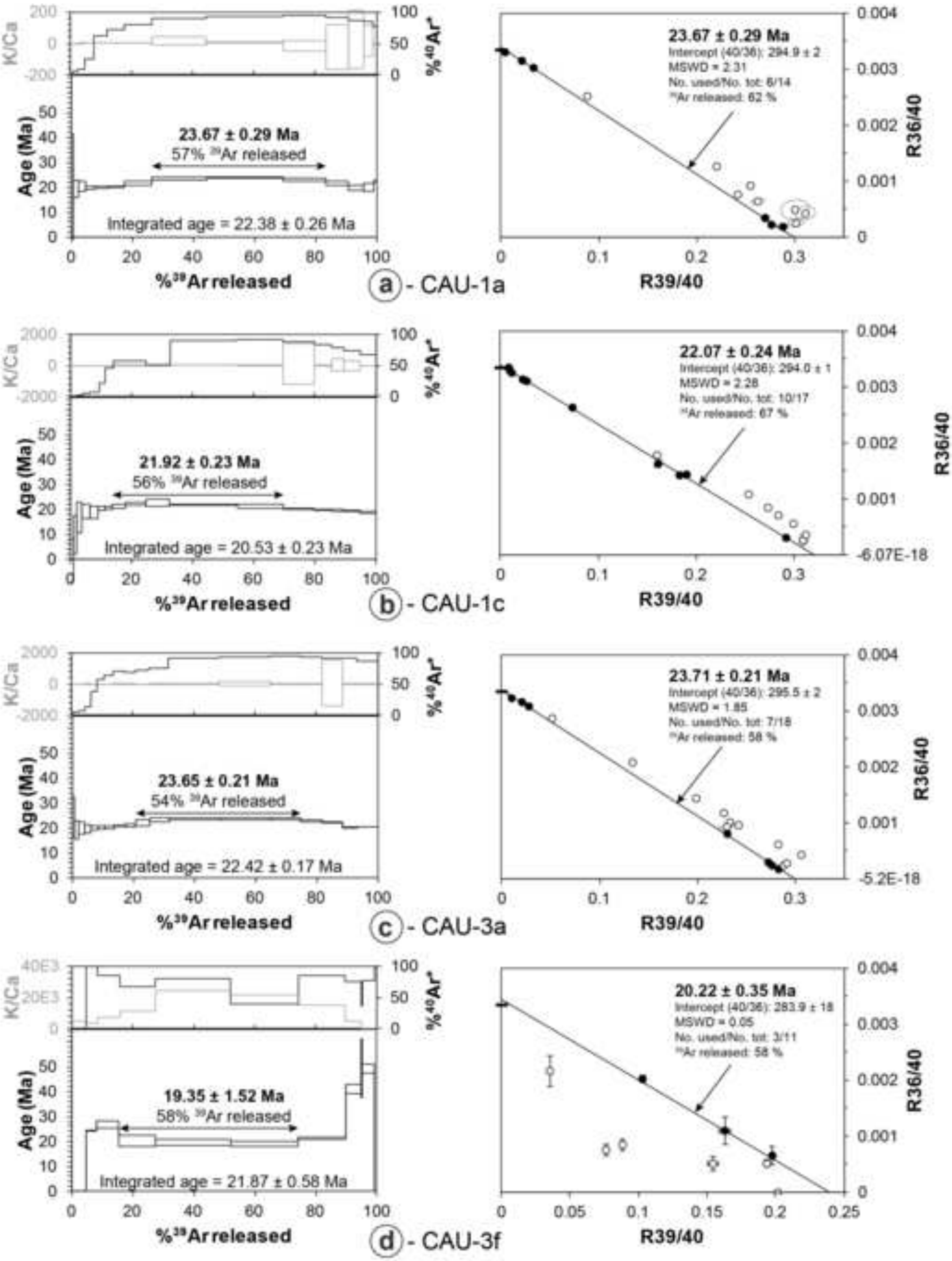

K/Ca
%40Ar*
Age (Ma)
23.67 ± 0.29 Ma
57% 39Ar released
Integrated age = 22.38 ± 0.26 Ma
%39Ar released
a - CAU-1a
23.67 ± 0.29 Ma
Intercept (40/36): 294.9 ± 2
MSWD = 2.31
No. used/No. tot: 6/14
39Ar released: 62 %
R39/40
R36/40
21.92 ± 0.23 Ma
56% 39Ar released
Integrated age = 20.53 ± 0.23 Ma
b - CAU-1c
22.07 ± 0.24 Ma
Intercept (40/36): 294.0 ± 1
MSWD = 2.28
No. used/No. tot: 10/17
39Ar released: 67 %
-6.07E-18
23.65 ± 0.21 Ma
54% 39Ar released
Integrated age = 22.42 ± 0.17 Ma
c - CAU-3a
23.71 ± 0.21 Ma
Intercept (40/36): 295.5 ± 2
MSWD = 1.85
No. used/No. tot: 7/18
39Ar released: 58 %
-5.2E-18
19.35 ± 1.52 Ma
58% 39Ar released
Integrated age = 21.87 ± 0.58 Ma
d - CAU-3f
20.22 ± 0.35 Ma
Intercept (40/36): 283.9 ± 18
MSWD = 0.05
No. used/No. tot: 3/11
39Ar released: 58 %


FIGURE. DR1-C

 

KMK-2 J = 0.00402950 ± 0.00000363

| Relative Abundances | | | 36Ar [V] | %1σ | 37Ar [V] | %1σ | 38Ar [V] | %1σ | 39Ar [V] | %1σ | 40Ar [V] | %1σ | 40(r)/39(k) ± 2σ | Age ± 2σ (Ma) | 40Ar(r) (%) | 39Ar(k) (%) | K/Ca ± 2σ |
|---|---|---|---|---|---|---|---|---|---|---|---|---|---|---|---|---|---|
| 48_KMK-2 | 4 °C | 4 | 1.1839652 | 0.511 | 231.8581 | 72.426 | 0.3215167 | 6.386 | 4.95915 | 0.668 | 371.0028 | 0.252 | 8.52452 ± 6.07881 | 61.07 ± 42.82 | 11.01 | 1.46 | 0.0089 ± 0.0129 |
| 49_KMK-2 | 4 °C | 4 | 0.5680986 | 0.691 | 134.9113 | 172.430 | 0.2579779 | 9.837 | 6.52910 | 0.550 | 201.6829 | 0.468 | 7.03545 ± 6.19151 | 50.55 ± 43.87 | 22.43 | 1.95 | 0.0205 ± 0.0707 |
| 51_KMK-2 | 5 °C | 4 | 0.2762329 | 1.149 | 265.9626 | 60.978 | 0.2666950 | 9.407 | 13.01527 | 0.628 | 148.9358 | 0.627 | 7.00618 ± 2.17753 | 50.34 ± 15.43 | 60.32 | 3.89 | 0.0207 ± 0.0253 |
| 52_KMK-2 | 5 °C | 4 | 0.0984086 | 3.023 | 303.8510 | 62.665 | 0.2356036 | 8.707 | 15.12151 | 0.301 | 107.7680 | 0.866 | 7.00719 ± 2.19461 | 50.35 ± 15.55 | 96.89 | 4.53 | 0.0211 ± 0.0264 |
| 53_KMK-2 | 5 °C | 4 | 0.0963079 | 3.187 | 216.0023 | 93.560 | 0.2716634 | 7.769 | 14.61645 | 0.193 | 114.3836 | 0.819 | 7.05201 ± 2.34370 | 50.67 ± 16.61 | 91.08 | 4.49 | 0.0288 ± 0.0539 |
| 55_KMK-2 | 6 °C | 4 | 0.0999899 | 2.979 | 29.7181 | 649.669 | 0.2428391 | 8.840 | 14.53952 | 0.185 | 121.8410 | 0.766 | 6.52232 ± 2.27418 | 46.91 ± 16.15 | 77.72 | 4.41 | 0.2101 ± 2.7294 |
| 56_KMK-2 | 6 °C | 4 | 0.1380666 | 2.228 | -169.60 | 90.823 | 0.6075632 | 4.609 | 44.83913 | 0.130 | 369.8846 | 0.260 | 6.83980 ± 0.57628 | 49.16 ± 4.09 | 84.95 | 13.95 | -0.1140 ± 0.2071 |
| 57_KMK-2 | 6 °C | 4 | 0.1912850 | 1.639 | 143.1068 | 85.817 | 1.3379733 | 1.752 | 100.95234 | 0.115 | 758.6071 | 0.123 | 6.92242 ± 0.20665 | 49.75 ± 1.46 | 94.03 | 31.30 | 0.3030 ± 0.5201 |
| 4_KMK-2_ | 7 °C | 4 | 0.0770691 | 11.247 | 294.5770 | 98.924 | 0.4479906 | 5.973 | 33.31179 | 0.128 | 219.7423 | 1.161 | 6.55654 ± 1.48708 | 47.15 ± 10.56 | 100.90 | 10.27 | 0.0483 ± 0.0956 |
| 5_KMK-2_ | 7 °C | 4 | 0.0584562 | 14.822 | 403.3393 | 72.429 | 0.2896831 | 11.745 | 21.71829 | 0.152 | 117.2863 | 2.176 | 6.26068 ± 2.35533 | 45.05 ± 16.74 | 114.37 | 6.51 | 0.0228 ± 0.0331 |
| 6_KMK-2_ | 8 °C | 4 | 0.0724425 | 12.081 | 617.6113 | 48.098 | 0.3092851 | 10.266 | 22.86000 | 0.140 | 114.7255 | 2.224 | 6.49998 ± 2.29767 | 46.75 ± 16.31 | 126.97 | 6.81 | 0.0156 ± 0.0150 |
| 8_KMK-2_ | 10 °C | 4 | 0.0912916 | 9.525 | 704.0786 | 40.752 | 0.3388404 | 7.878 | 21.13750 | 0.219 | 103.3896 | 2.469 | 6.60114 ± 2.41926 | 47.47 ± 17.17 | 131.69 | 6.27 | 0.0126 ± 0.0103 |
| 9_KMK-2_ | 12 °C | 4 | 0.0525406 | 16.497 | 573.1992 | 66.571 | 0.2170933 | 14.152 | 14.13494 | 0.357 | 76.3872 | 3.342 | 7.98376 ± 4.79143 | 57.26 ± 33.83 | 143.38 | 4.17 | 0.0103 ± 0.0137 |
| | | Σ | 3.0041547 | 0.734 | 3748.6166 | 23.075 | 5.1447248 | 1.833 | 327.73499 | 0.060 | 2825.6367 | 0.223 | | | | | |

KPA-8 J = 0.0039438 ± 0.00000355

| Relative Abundances | | | 36Ar [V] | %1σ | 37Ar [V] | %1σ | 38Ar [V] | %1σ | 39Ar [V] | %1σ | 40Ar [V] | %1σ | 40(r)/39(k) ± 2σ | Age ± 2σ (Ma) | 40Ar(r) (%) | 39Ar(k) (%) | K/Ca ± 2σ |
|---|---|---|---|---|---|---|---|---|---|---|---|---|---|---|---|---|---|
| 31_KPA-8 | 3 °C | | 2.8089159 | 0.536 | 234.32 | 130.296 | 0.6593686 | 3.542 | 3.20068 | 0.820 | 843.8298 | 0.072 | 11.13103 ± 17.59558 | 77.69 ± 120.21 | 4.00 | 1.52 | 0.0056 ± 0.0145 |
| 32_KPA-8 | 4 °C | | 2.6898971 | 0.550 | 195.28 | 150.750 | 0.6711098 | 4.116 | 7.48457 | 0.411 | 829.3414 | 0.068 | 7.10266 ± 7.13672 | 49.96 ± 49.51 | 6.15 | 3.61 | 0.0162 ± 0.0488 |
| 33_KPA-8 | 4 °C | 4 | 1.7738239 | 0.533 | 261.41 | 118.841 | 0.5120498 | 5.930 | 10.48252 | 0.495 | 574.4086 | 0.096 | 7.18749 ± 5.30643 | 50.55 ± 36.80 | 12.60 | 5.06 | 0.0169 ± 0.0402 |
| 35_KPA-8 | 5 °C | 4 | 0.4962284 | 0.761 | 97.74 | 380.046 | 0.2574942 | 9.157 | 13.08041 | 0.307 | 212.9395 | 0.259 | 5.85080 ± 4.97662 | 41.25 ± 34.69 | 34.98 | 6.40 | 0.0572 ± 0.4350 |
| 36_KPA-8 | 5 °C | 4 | 0.2897844 | 0.903 | 213.48 | 232.238 | 0.2457546 | 6.535 | 11.22189 | 0.282 | 142.6239 | 0.386 | 6.78306 ± 7.64231 | 47.74 ± 53.08 | 52.63 | 5.56 | 0.0223 ± 0.1035 |
| 37_KPA-8 | 5 °C | 4 | 0.3112543 | 0.847 | 130.12 | 250.994 | 0.2640977 | 12.342 | 12.42831 | 0.238 | 162.4586 | 0.337 | 6.60376 ± 4.51844 | 46.49 ± 31.41 | 50.14 | 6.20 | 0.0408 ± 0.2046 |
| 39_KPA-8 | 5 °C | 4 | 0.1868086 | 1.810 | 23.81 | 913.916 | 0.9692660 | 2.109 | 71.99564 | 0.134 | 593.5181 | 0.148 | 7.49733 ± 0.51736 | 52.69 ± 3.58 | 90.92 | 36.17 | 1.2999 ± 23.7605 |
| 40_KPA-8 | 6 °C | 4 | 0.0683805 | 3.439 | -745.35 | 46.385 | 0.3885421 | 7.195 | 32.44277 | 0.200 | 364.3965 | 0.454 | 8.68685 ± 1.84452 | 60.91 ± 12.72 | 76.96 | 16.22 | -0.0190 ± 0.0177 |
| 41_KPA-8 | 6 °C | | 0.0430701 | 2.523 | -813.85 | 69.654 | 0.1578973 | 15.361 | 12.94441 | 0.371 | 248.4135 | 0.063 | 12.55212 ± 7.34728 | 87.37 ± 49.93 | 66.94 | 6.66 | -0.0072 ± 0.0100 |
| 43_KPA-8 | 6 °C | | 0.0425698 | 2.407 | -572.74 | 96.309 | 0.1136482 | 26.458 | 8.10058 | 0.637 | 181.0269 | 0.085 | 14.35041 ± 11.36444 | 99.55 ± 76.71 | 66.08 | 4.19 | -0.0064 ± 0.0123 |
| 44_KPA-8 | 7 °C | | 0.0562862 | 1.242 | -483.32 | 65.192 | 0.1757371 | 11.013 | 9.27267 | 0.519 | 174.7342 | 0.091 | 12.14450 ± 5.62442 | 84.60 ± 38.28 | 66.89 | 4.84 | -0.0086 ± 0.0112 |
| 45_KPA-8 | 8 °C | | 0.0601309 | 1.322 | -240.19 | 109.146 | 0.1056815 | 20.501 | 7.09495 | 0.579 | 172.0936 | 0.089 | 18.80735 ± 6.36101 | 129.39 ± 42.23 | 77.76 | 3.58 | -0.0130 ± 0.0284 |
| | | Σ | 8.8271500 | 0.273 | -1699.29 | 77.343 | 4.5206470 | 1.934 | 199.74940 | 0.087 | 4499.7847 | 0.052 | | | | | |

**TABLE DR2**

Suppl. file_Table DR3

Click here to download Supplemental file Supl. file_Table. DR3.xlsx

CAU-1a J=0.00395580±0.0000047! Spectro : ARGUS IV

| Relative Abundances | | 36Ar [fA] | %1s | 37Ar [fA] | %1s | 38Ar [fA] | %1s | 39Ar [fA] | %1s | 40Ar [fA] | %1s | 40*/39(k) ± 2s | Age ± 2s (Ma) | 40Ar* (%) | 39Ar(k) (%) | K/Ca ± 2s |
|---|---|---|---|---|---|---|---|---|---|---|---|---|---|---|---|---|
| 18 CAU1A | 3.0 % | 4.516016 | 0.477 | 43.54992 | 5.860 | 1.365495 | 1.126 | 5.61404 | 0.644 | 1360.5627 | 0.255 | 2.85746 ± 2.99338 | 20.28 ± 21.12 | 1.17 | 0.60 | 0.06 ± 0.01 |
| 20 CAU1A | 3.5 % | 2.272683 | 0.432 | 36.60379 | 12.817 | 0.890510 | 1.677 | 15.25865 | 0.155 | 717.1486 | 0.072 | 2.73215 ± 0.47587 | 19.39 ± 3.36 | 5.80 | 1.65 | 0.18 ± 0.05 |
| 21 CAU1A | 4.0 % | 2.050184 | 0.393 | 34.64924 | 13.773 | 0.883057 | 1.870 | 22.40054 | 0.164 | 673.5708 | 0.076 | 2.87059 ± 0.27648 | 20.37 ± 1.95 | 9.54 | 2.42 | 0.28 ± 0.08 |
| 22 CAU1A | 4.5 % | 0.763622 | 0.466 | 18.26025 | 24.101 | 0.678404 | 3.097 | 26.48788 | 0.128 | 41967.0000 | 0.170 | 2.80282 ± 0.10697 | 19.89 ± 0.76 | 24.66 | 2.87 | 0.62 ± 0.30 |
| 24 CAU1A | 5.0 % | 0.235595 | 1.038 | 18.60246 | 23.769 | 0.653277 | 2.811 | 39.92276 | 0.101 | 181.5618 | 0.275 | 2.81728 ± 0.04966 | 19.99 ± 0.35 | 61.93 | 4.32 | 0.92 ± 0.44 |
| 25 CAU1A | 5.3 % | 0.191578 | 1.253 | 17.25970 | 27.923 | 0.768086 | 2.162 | 51.32276 | 0.097 | 201.9357 | 0.263 | 2.84008 ± 0.03928 | 20.16 ± 0.28 | 72.16 | 5.56 | 1.28 ± 0.72 |
| 26 CAU1A | 5.6 % | 0.210138 | 3.758 | 14.00596 | 25.408 | 1.143705 | 1.627 | 83.77487 | 0.099 | 320.1243 | 1.220 | 3.07741 ± 0.10942 | 21.83 ± 0.77 | 80.52 | 9.07 | 2.57 ± 1.32 |
| 28 CAU1A | 5.9 % | 0.214924 | 8.727 | 4.18793 | 83.477 | 2.219469 | 2.132 | 164.39158 | 0.101 | 610.8941 | 0.773 | 3.31832 ± 0.08947 | 23.53 ± 0.63 | 89.29 | 17.81 | 16.88 ± 28.21 |
| 29 CAU1A | 6.2 % | 0.200666 | 9.468 | 23.74601 | 29.916 | 3.053111 | 1.986 | 232.17280 | 0.095 | 842.4791 | 0.263 | 3.36998 ± 0.05313 | 23.89 ± 0.37 | 92.86 | 25.15 | 4.20 ± 2.54 |
| 30 CAU1A | 6.5 % | 0.085851 | 12.755 | -3.16533 | 90.190 | 1.692738 | 1.080 | 128.77458 | 0.096 | 448.2447 | 1.051 | 3.26994 ± 0.08935 | 23.19 ± 0.63 | 93.94 | 13.95 | -17.49 ± 31.59 |
| 32 CAU1A | 6.8 % | 0.058090 | 13.479 | -1.21155 | 291.762 | 0.891483 | 3.860 | 68.16303 | 0.103 | 226.8244 | 1.264 | 3.06198 ± 0.10910 | 21.72 ± 0.77 | 92.02 | 7.38 | -24.19 ± 141.18 |
| 33 CAU1A | 7.1 % | 0.062935 | 13.683 | 0.72994 | 342.136 | 0.629049 | 3.290 | 45.41806 | 0.111 | 146.5107 | 1.637 | 2.80384 ± 0.15528 | 19.90 ± 1.10 | 86.92 | 4.92 | 26.75 ± 183.09 |
| 34 CAU1A | 7.5 % | 0.049687 | 17.355 | 0.84383 | 320.119 | 0.413439 | 5.188 | 29.82742 | 0.126 | 99.5771 | 2.409 | 2.83390 ± 0.23659 | 20.11 ± 1.67 | 84.89 | 3.23 | 15.20 ± 97.32 |
| 36 CAU1A | 8.0 % | 0.030373 | 1.549 | -1.78502 | 106.081 | 0.205951 | 5.066 | 9.72380 | 0.186 | 40.2830 | 0.133 | 3.18423 ± 0.04745 | 22.58 ± 0.33 | 76.87 | 1.05 | -2.34 ± 4.97 |
| | S | 10.942342 | 0.383 | 206.27712 | 7.297 | 15.487774 | 0.664 | 923.25278 | 0.037 | 6170.5939 | 0.160 | | | | | |

CAU-1c J=0.00395580±0.0000047! Spectro : ARGUS IV

| Relative Abundances | | 36Ar [fA] | %1s | 37Ar [fA] | %1s | 38Ar [fA] | %1s | 39Ar [fA] | %1s | 40Ar [fA] | %1s | 40(r)/39(k) ± 2s | Age ± 2s (Ma) | 40Ar(r) (%) | 39Ar(k) (%) | K/Ca ± 2s |
|---|---|---|---|---|---|---|---|---|---|---|---|---|---|---|---|---|
| 06 CAU1C | 3.0 % | 2.955930 | 0.415 | 36.55443 | 4.950 | 1.188579 | 1.545 | 7.49918 | 0.219 | 879.1289 | 0.049 | -0.04320 ± 1.21342 | -0.31 ± 8.66 | -0.04 | 0.88 | 0.09 ± 0.01 |
| 08 CAU1C | 3.5 % | 3.301567 | 0.406 | 31.94784 | 3.601 | 1.261587 | 1.337 | 9.28493 | 0.281 | 995.9706 | 0.048 | 1.39414 ± 1.07867 | 9.92 ± 7.66 | 1.30 | 1.09 | 0.12 ± 0.01 |
| 09 CAU1C | 4.0 % | 4.366770 | 0.407 | 37.89264 | 3.444 | 1.446225 | 1.452 | 15.46007 | 0.135 | 1336.8954 | 0.036 | 2.34966 ± 0.85575 | 16.69 ± 6.05 | 2.71 | 1.81 | 0.18 ± 0.02 |
| 010 CAU1( | 4.5 % | 2.905542 | 0.406 | 29.32351 | 4.520 | 1.096971 | 1.101 | 21.11387 | 0.134 | 922.4625 | 0.050 | 2.71663 ± 0.41727 | 19.28 ± 2.95 | 6.21 | 2.48 | 0.31 ± 0.04 |
| 012 CAU1( | 5.0 % | 2.808190 | 0.412 | 21.32195 | 6.432 | 1.081115 | 1.994 | 24.04572 | 0.140 | 900.7403 | 0.047 | 2.66030 ± 0.35754 | 18.89 ± 2.53 | 7.10 | 2.83 | 0.48 ± 0.07 |
| 013 CAU1( | 5.3 % | 0.682495 | 0.508 | 7.84246 | 28.831 | 0.438070 | 4.678 | 18.96641 | 0.189 | 257.9112 | 0.158 | 2.88154 ± 0.13577 | 20.45 ± 0.96 | 21.18 | 2.23 | 1.04 ± 0.61 |
| 014 CAU1( | 5.6 % | 0.233447 | 0.730 | 11.09798 | 11.352 | 0.336339 | 6.030 | 20.62905 | 0.159 | 129.0176 | 0.331 | 2.91325 ± 0.06890 | 20.67 ± 0.49 | 46.56 | 2.43 | 0.80 ± 0.19 |
| 4_CAU1C_ | 5.9 % | 0.285420 | 2.334 | 4.93811 | 52.818 | 0.611927 | 5.553 | 37.44759 | 0.124 | 197.2739 | 0.741 | 2.99436 ± 0.13332 | 21.24 ± 0.94 | 56.84 | 4.40 | 3.26 ± 3.45 |
| 5_CAU1C_ | 6.2 % | 0.427052 | 1.686 | 5.19248 | 70.435 | 0.909102 | 4.496 | 54.41640 | 0.102 | 297.7087 | 0.237 | 3.12662 ± 0.08535 | 22.18 ± 0.60 | 57.15 | 6.40 | 4.51 ± 6.36 |
| 6_CAU1C_ | 6.5 % | 0.683213 | 1.694 | 17.30755 | 11.221 | 1.187802 | 3.433 | 66.87030 | 0.104 | 415.6859 | 1.341 | 3.17908 ± 0.19716 | 22.55 ± 1.39 | 51.13 | 7.86 | 1.66 ± 0.40 |
| 8_CAU1C_ | 6.8 % | 0.207712 | 5.554 | 5.09086 | 41.333 | 2.817174 | 1.039 | 189.33288 | 0.102 | 650.6676 | 0.141 | 3.10177 ± 0.03826 | 22.00 ± 0.27 | 90.25 | 22.27 | 15.99 ± 13.28 |
| 9_CAU1C_ | 7.1 % | 0.114870 | 19.203 | 13.93231 | 29.290 | 1.743316 | 2.087 | 126.98796 | 0.106 | 411.8709 | 0.669 | 2.97330 ± 0.11276 | 21.10 ± 0.80 | 91.67 | 14.93 | 3.92 ± 2.32 |
| 10_CAU1C | 7.4 % | 0.102980 | 3.803 | 0.35399 | 621.535 | 1.155650 | 3.393 | 87.29553 | 0.114 | 280.5889 | 0.325 | 2.85271 ± 0.03494 | 20.24 ± 0.25 | 88.75 | 10.27 | 106.04 ± 1318.18 |
| 12_CAU1C | 7.7 % | 0.090989 | 2.165 | -1.95185 | 133.733 | 0.698318 | 2.792 | 48.22579 | 0.107 | 161.5814 | 0.338 | 2.77397 ± 0.03523 | 19.69 ± 0.25 | 82.79 | 5.67 | -10.62 ± 28.43 |
| 13_CAU1C | 8.0 % | 0.081707 | 2.296 | 0.47047 | 666.908 | 0.499815 | 5.382 | 32.40767 | 0.108 | 114.4076 | 0.478 | 2.76912 ± 0.05165 | 19.65 ± 0.36 | 78.44 | 3.81 | 29.62 ± 395.08 |
| 14_CAU1C | 9.0 % | 0.141869 | 1.402 | -0.53409 | 444.453 | 0.695800 | 2.822 | 45.50024 | 0.106 | 166.9138 | 0.328 | 2.72679 ± 0.03747 | 19.36 ± 0.26 | 74.33 | 5.35 | -36.63 ± 325.65 |
| 16_CAU1C | 12.0 % | 0.191802 | 1.179 | -6.29791 | 38.434 | 0.747016 | 2.177 | 45.00317 | 0.108 | 177.7849 | 0.307 | 2.65605 ± 0.04085 | 18.86 ± 0.29 | 67.24 | 5.29 | -3.07 ± 2.37 |
| | S | 19.581555 | 0.218 | 214.48272 | 4.536 | 17.914806 | 0.623 | 850.48676 | 0.035 | 8296.6101 | 0.081 | | | | | |

CAU-3a J=0.00395580±0.0000047! Spectro : ARGUS IV

| Relative Abundances | | 36Ar [fA] | %1s | 37Ar [fA] | %1s | 38Ar [fA] | %1s | 39Ar [fA] | %1s | 40Ar [fA] | %1s | 40*/39(k) ± 2s | Age ± 2s (Ma) | 40Ar* (%) | 39Ar(k) (%) | K/Ca ± 2s |
|---|---|---|---|---|---|---|---|---|---|---|---|---|---|---|---|---|
| 18 CAU3A | 3.5 % | 2.2527018 | 0.466 | 17.64813 | 36.203 | 0.714955 | 2.749 | 7.1070 | 0.289 | 695.7188 | 0.189 | 3.46778 ± 1.12519 | 24.58 ± 7.92 | 3.54 | 0.70 | 0.17 ± 0.13 |
| 20 CAU3A | 4.0 % | 2.1473180 | 0.427 | 15.14025 | 28.344 | 0.854097 | 3.415 | 14.0449 | 0.161 | 677.8913 | 0.163 | 2.70444 ± 0.50482 | 19.20 ± 3.56 | 5.60 | 1.38 | 0.40 ± 0.23 |
| 21 CAU3A | 4.5 % | 2.2260178 | 0.389 | 22.16793 | 18.988 | 0.862905 | 2.126 | 20.0461 | 0.110 | 719.9477 | 0.153 | 2.84873 ± 0.34578 | 20.22 ± 2.44 | 7.93 | 1.97 | 0.39 ± 0.15 |
| 22 CAU3A | 5.0 % | 1.1741790 | 0.560 | 3.07897 | 190.743 | 0.616350 | 3.261 | 21.0334 | 0.122 | 408.6987 | 0.286 | 2.76716 ± 0.24398 | 19.64 ± 1.72 | 14.24 | 2.07 | 2.94 ± 11.21 |
| 24 CAU3A | 5.3 % | 0.3310181 | 1.105 | 14.55382 | 29.578 | 0.406194 | 5.047 | 20.9485 | 0.142 | 156.9493 | 0.196 | 2.82593 ± 0.11763 | 20.06 ± 0.83 | 37.70 | 2.06 | 0.62 ± 0.37 |
| 25 CAU3A | 5.6 % | 0.1839528 | 1.726 | 11.83707 | 39.537 | 0.427402 | 5.587 | 24.8448 | 0.136 | 125.2538 | 0.253 | 2.86316 ± 0.08810 | 20.32 ± 0.62 | 56.77 | 2.45 | 0.90 ± 0.72 |
| 26 CAU3A | 5.9 % | 0.1562779 | 2.069 | -6.68326 | 67.802 | 0.428279 | 4.903 | 30.3017 | 0.121 | 133.8858 | 0.225 | 2.84952 ± 0.07246 | 20.22 ± 0.51 | 64.50 | 2.99 | -1.95 ± 2.65 |
| 28 CAU3A | 6.2 % | 0.1465956 | 2.680 | 4.39217 | 88.759 | 0.555135 | 3.871 | 36.4632 | 0.111 | 151.0139 | 0.473 | 2.94214 ± 0.07815 | 20.88 ± 0.55 | 71.03 | 3.59 | 3.57 ± 6.34 |
| 29 CAU3A | 6.5 % | 0.1582600 | 2.540 | 9.51032 | 43.392 | 0.537045 | 2.946 | 35.6433 | 0.105 | 153.2633 | 0.456 | 2.98811 ± 0.08107 | 21.20 ± 0.57 | 69.48 | 3.51 | 1.61 ± 1.40 |
| 30 CAU3A | 6.8 % | 0.1910077 | 1.264 | 12.70945 | 23.217 | 0.664209 | 2.160 | 46.0625 | 0.106 | 200.5556 | 1.876 | 3.13061 ± 0.16705 | 22.20 ± 1.18 | 71.89 | 4.54 | 1.56 ± 0.73 |
| 32 CAU3A | 7.2 % | 0.2322562 | 3.873 | 9.80682 | 28.757 | 0.933880 | 4.641 | 65.1650 | 0.152 | 283.3798 | 0.571 | 3.28815 ± 0.09724 | 23.31 ± 0.69 | 75.60 | 6.42 | 2.86 ± 1.66 |
| 33 CAU3A | 7.5 % | 0.1868738 | 8.660 | 3.36755 | 68.413 | 2.260665 | 1.948 | 167.8381 | 0.088 | 617.6648 | 0.075 | 3.33978 ± 0.05822 | 23.68 ± 0.41 | 90.75 | 16.54 | 21.43 ± 29.37 |
| 34 CAU3A | 7.8 % | 0.1520246 | 2.920 | 2.24741 | 171.304 | 2.226168 | 0.771 | 169.8242 | 0.073 | 616.4084 | 0.579 | 3.35390 ± 0.04533 | 23.78 ± 0.32 | 92.40 | 16.73 | 32.49 ± 111.35 |
| 36 CAU3A | 8.5 % | 0.0639352 | 13.956 | 2.48021 | 130.478 | 1.305095 | 3.360 | 99.4785 | 0.121 | 352.4664 | 0.129 | 3.34377 ± 0.05523 | 23.71 ± 0.39 | 94.37 | 9.80 | 17.25 ± 45.03 |
| 37 CAU3A | 9.0 % | 0.0590189 | 15.080 | -2.56009 | 130.499 | 0.978539 | 4.451 | 72.3497 | 0.139 | 252.4294 | 0.179 | 3.23266 ± 0.07548 | 22.92 ± 0.53 | 92.65 | 7.13 | -12.15 ± 31.73 |
| 38 CAU3A | 9.0 % | 0.0655049 | 4.850 | 0.42226 | 1074.174 | 0.934827 | 2.873 | 66.3406 | 0.088 | 228.2513 | 0.256 | 3.13667 ± 0.03605 | 22.25 ± 0.25 | 91.17 | 6.54 | 67.56 ± 1451.36 |
| 40 CAU3A | 10.0 % | 0.0718457 | 3.673 | 4.55087 | 53.924 | 0.792799 | 3.688 | 49.2345 | 0.126 | 161.2931 | 0.255 | 2.83879 ± 0.03787 | 20.15 ± 0.27 | 86.65 | 4.85 | 4.65 ± 5.03 |
| 41 CAU3A | 12.0 % | 0.1531753 | 1.703 | 10.99301 | 31.140 | 1.058174 | 3.460 | 68.2344 | 0.102 | 242.1234 | 0.171 | 2.88269 ± 0.02816 | 20.46 ± 0.20 | 81.23 | 6.72 | 2.67 ± 1.68 |
| | S | 9.9519632 | 0.306 | 135.66289 | 12.797 | 16.556718 | 0.744 | 1014.9604 | 0.030 | 6177.1947 | 0.099 | | | | | |

**TABLE DR3**

| NAV-3b | J=0.00402950±0.00000: Spectro : ARGUS IV | | | | | | | | | | | | | | | |
|---|---|---|---|---|---|---|---|---|---|---|---|---|---|---|---|---|
| **Relative Abundances** | | 36Ar [V] | %1s | 37Ar [V] | %1s | 38Ar [V] | %1s | 39Ar [V] | %1s | 40Ar [V] | %1s | 40*/39(k) ± 2s | Age ± 2s (Ma) | 40Ar* (%) | 39Ar(k) (%) | K/Ca ± 2s |
| 9_NAV-3B | 4.0% | 24.071859 | 0.571 | 974.8500 | 3.800 | 6.452027 | 0.489 | 29.2382 | 0.264 | 7129.981 | 0.048 | 3.49467 ± 3.35953 | 25.29 ± 24.14 | 1.40 | 1.97 | 0.013 ± 0.001 |
| 10_NAV-3 | 5.0% | 11.580366 | 0.574 | 648.5615 | 5.972 | 3.480601 | 0.789 | 32.7046 | 0.237 | 3580.652 | 0.083 | 6.62952 ± 1.45997 | 47.67 ± 10.36 | 5.97 | 2.23 | 0.021 ± 0.003 |
| 12_NAV-3 | 5.5% | 3.903645 | 0.616 | 440.0984 | 9.459 | 1.590267 | 1.424 | 37.1487 | 0.213 | 1332.082 | 0.227 | 5.85733 ± 0.52065 | 42.18 ± 3.71 | 16.19 | 2.55 | 0.036 ± 0.007 |
| 13_NAV-3 | 6.0% | 1.468001 | 0.768 | 261.4635 | 33.774 | 0.998112 | 1.998 | 41.1356 | 0.212 | 651.098 | 0.458 | 5.84172 ± 0.43820 | 42.07 ± 3.12 | 36.74 | 2.83 | 0.067 ± 0.045 |
| 14_NAV-3 | 6.3% | 0.626130 | 1.393 | 225.9253 | 12.936 | 0.901243 | 2.375 | 45.2578 | 0.204 | 420.622 | 0.721 | 5.64217 ± 0.21635 | 40.65 ± 1.54 | 60.49 | 3.12 | 0.086 ± 0.022 |
| 16_NAV-3 | 6.6% | 0.450185 | 1.795 | 79.9672 | 112.109 | 0.649674 | 3.459 | 35.6219 | 0.236 | 327.276 | 0.914 | 5.64410 ± 0.48233 | 40.67 ± 3.44 | 61.33 | 2.46 | 0.191 ± 0.429 |
| 17_NAV-3 | 6.9% | 0.391032 | 2.037 | 142.1313 | 56.491 | 0.620744 | 3.355 | 33.6207 | 0.222 | 311.508 | 0.958 | 6.19825 ± 0.47011 | 44.61 ± 3.34 | 66.69 | 2.32 | 0.101 ± 0.115 |
| 18_NAV-3 | 7.2% | 0.383583 | 2.104 | 36.5946 | 75.686 | 0.679554 | 3.692 | 38.3892 | 0.211 | 344.616 | 0.885 | 6.10043 ± 0.23878 | 43.91 ± 1.70 | 67.91 | 2.65 | 0.451 ± 0.682 |
| 20_NAV-3 | 7.5% | 0.617538 | 1.367 | -31.8060 | 80.778 | 1.253744 | 1.678 | 78.9865 | 0.162 | 680.972 | 0.443 | 6.26551 ± 0.11657 | 45.09 ± 0.83 | 72.70 | 5.46 | -1.068 ± 1.726 |
| 21_NAV-3 | 7.8% | 0.845306 | 5.636 | 17.6699 | 160.546 | 2.497727 | 1.983 | 170.3464 | 0.155 | 1357.707 | 0.693 | 6.50367 ± 0.20211 | 46.78 ± 1.44 | 81.59 | 11.77 | 4.145 ± 13.310 |
| 22_NAV-3 | 8.1% | 1.375291 | 5.032 | 30.9040 | 95.668 | 6.908670 | 1.099 | 507.1068 | 0.144 | 3567.849 | 0.541 | 6.23009 ± 0.11296 | 44.84 ± 0.80 | 88.55 | 35.05 | 7.056 ± 13.500 |
| 24_NAV-3 | 8.4% | 0.427832 | 1.741 | 123.3786 | 33.397 | 1.980591 | 1.118 | 144.0581 | 0.143 | 941.179 | 0.185 | 5.72255 ± 0.06529 | 41.22 ± 0.47 | 87.54 | 9.95 | 0.502 ± 0.335 |
| 25_NAV-3 | 8.7% | 0.347291 | 2.174 | 49.9188 | 77.368 | 1.043066 | 2.383 | 69.6635 | 0.161 | 458.658 | 0.478 | 5.16493 ± 0.13201 | 37.25 ± 0.94 | 78.41 | 4.81 | 0.600 ± 0.928 |
| 26_NAV-3 | 9.0% | 0.273815 | 2.708 | 2.3805 | 946.327 | 0.670710 | 3.440 | 47.3429 | 0.189 | 301.250 | 0.728 | 4.64885 ± 0.15548 | 33.56 ± 1.11 | 73.06 | 3.27 | 8.551 ± 161.850 |
| 28_NAV-3 | 10.0% | 0.424388 | 1.799 | 43.4034 | 57.291 | 0.923435 | 2.180 | 61.7075 | 0.173 | 406.348 | 0.539 | 4.60544 ± 0.12494 | 33.25 ± 0.89 | 69.90 | 4.26 | 0.611 ± 0.700 |
| 29_NAV-3 | 12.0% | 0.597971 | 1.363 | -2.0230 | 1208.846 | 1.190922 | 2.100 | 76.8151 | 0.165 | 517.295 | 0.424 | 4.42211 ± 0.10297 | 31.94 ± 0.74 | 65.67 | 5.31 | -16.328 ± 394.761 |
| | S | 47.784230 | 0.373 | 3043.4182 | 6.214 | 31.841089 | 0.397 | 1449.1435 | 0.060 | 22329.092 | 0.107 | | | | | |

| NAV-3c | J=0.00402950±0.00000: Spectro : ARGUS IV | | | | | | | | | | | | | | | |
|---|---|---|---|---|---|---|---|---|---|---|---|---|---|---|---|---|
| **Relative Abundances** | | 36Ar [V] | %1s | 37Ar [V] | %1s | 38Ar [V] | %1s | 39Ar [V] | %1s | 40Ar [V] | %1s | 40(r)/39(k) ± 2s | Age ± 2s (Ma) | 40Ar(r) (%) | 39Ar(k) (%) | K/Ca ± 2s |
| 30_NAV-3 | 4.0% | 8.752647 | 0.596 | 426.7565 | 8.165 | 2.514326 | 1.690 | 13.5829 | 0.722 | 2603.852 | 0.128 | 4.05000 ± 2.78278 | 29.27 ± 19.95 | 2.06 | 1.15 | 0.013 ± 0.002 |
| 33_NAV-3 | 5.0% | 11.214253 | 0.583 | 585.3519 | 5.546 | 3.508387 | 1.328 | 33.1208 | 0.329 | 3477.948 | 0.095 | 6.53924 ± 1.40857 | 47.03 ± 10.00 | 6.15 | 2.83 | 0.024 ± 0.003 |
| 34_NAV-3 | 5.5% | 2.908345 | 0.749 | 363.0345 | 9.858 | 1.302245 | 2.816 | 25.2080 | 0.399 | 989.550 | 0.338 | 6.44893 ± 0.68821 | 46.39 ± 4.89 | 16.26 | 2.16 | 0.030 ± 0.006 |
| 35_NAV-3 | 6.0% | 1.394728 | 1.125 | 296.6431 | 15.241 | 0.865514 | 4.489 | 26.5601 | 0.387 | 549.448 | 0.614 | 6.16229 ± 0.54708 | 44.35 ± 3.89 | 29.55 | 2.28 | 0.038 ± 0.012 |
| 37_NAV-3 | 6.3% | 0.530153 | 2.671 | 210.5173 | 22.268 | 0.707024 | 4.914 | 31.4310 | 0.456 | 319.566 | 1.060 | 5.77253 ± 0.43768 | 41.58 ± 3.12 | 56.50 | 2.71 | 0.064 ± 0.028 |
| 38_NAV-3 | 6.6% | 0.335936 | 4.083 | 277.1481 | 24.569 | 0.528844 | 6.699 | 26.4947 | 0.450 | 241.116 | 1.412 | 6.28306 ± 0.60876 | 45.21 ± 4.33 | 68.52 | 2.28 | 0.041 ± 0.020 |
| 39_NAV-3 | 6.9% | 0.241142 | 5.628 | 141.6432 | 27.439 | 0.412575 | 9.544 | 21.1454 | 1.127 | 190.018 | 1.741 | 6.20784 ± 0.60618 | 44.68 ± 4.31 | 68.74 | 1.82 | 0.064 ± 0.035 |
| 41_NAV-3 | 7.2% | 0.242656 | 5.559 | 143.1868 | 33.818 | 0.448551 | 8.689 | 26.2855 | 0.391 | 224.302 | 1.491 | 6.28464 ± 0.51255 | 45.22 ± 3.64 | 73.36 | 2.27 | 0.079 ± 0.053 |
| 42_NAV-3 | 7.5% | 0.329281 | 4.115 | 92.9742 | 36.342 | 0.553563 | 6.936 | 27.9930 | 0.392 | 269.873 | 1.226 | 6.45414 ± 0.43010 | 46.43 ± 3.05 | 66.78 | 2.42 | 0.129 ± 0.094 |
| 43_NAV-3 | 7.8% | 0.479685 | 2.867 | 19.0977 | 187.128 | 0.831439 | 4.518 | 46.1147 | 0.251 | 435.650 | 0.758 | 6.40131 ± 0.26571 | 46.05 ± 1.89 | 67.74 | 4.00 | 1.038 ± 3.885 |
| 45_NAV-3 | 8.1% | 0.382928 | 3.562 | 27.6454 | 116.220 | 0.714079 | 5.614 | 44.3478 | 0.257 | 406.026 | 0.814 | 6.65059 ± 0.26851 | 47.82 ± 1.91 | 72.61 | 3.84 | 0.689 ± 1.603 |
| 46_NAV-3 | 8.3% | 0.441581 | 7.202 | -103.9544 | 75.409 | 1.527758 | 2.373 | 108.2819 | 0.178 | 879.165 | 0.975 | 6.81805 ± 0.26662 | 49.01 ± 1.89 | 84.03 | 9.39 | -0.448 ± 0.676 |
| 47_NAV-3 | 8.6% | 0.825150 | 3.863 | 17.7697 | 164.163 | 5.198367 | 0.801 | 390.9425 | 0.145 | 2804.071 | 0.284 | 6.54328 ± 0.06727 | 47.06 ± 0.48 | 91.22 | 33.89 | 9.460 ± 31.059 |
| 4_NAV-3C | 9.0% | 0.296675 | 10.789 | 66.4975 | 76.241 | 1.840361 | 1.671 | 134.9982 | 0.165 | 909.669 | 0.845 | 6.12346 ± 0.19278 | 44.08 ± 1.37 | 90.84 | 11.70 | 0.873 ± 1.331 |
| 5_NAV-3C | 9.5% | 0.274793 | 9.852 | 105.6833 | 37.942 | 1.096781 | 2.486 | 79.8466 | 0.224 | 497.948 | 1.437 | 5.32747 ± 0.28379 | 38.41 ± 2.02 | 85.34 | 6.91 | 0.325 ± 0.246 |
| 6_NAV-3C | 10.0% | 0.265903 | 10.089 | 38.1470 | 42.728 | 0.770335 | 2.495 | 53.8095 | 0.283 | 325.930 | 2.196 | 4.65000 ± 0.40155 | 33.57 ± 2.87 | 76.73 | 4.66 | 0.606 ± 0.518 |
| 8_NAV-3C | 12.0% | 0.370818 | 7.520 | 48.8411 | 48.762 | 1.023809 | 2.959 | 65.5177 | 0.249 | 401.063 | 1.788 | 4.50543 ± 0.34034 | 32.53 ± 2.44 | 73.56 | 5.68 | 0.577 ± 0.562 |
| | S | 29.286675 | 0.408 | 2756.9828 | 6.462 | 23.843957 | 0.634 | 1155.6803 | 0.071 | 15525.196 | 0.140 | | | | | |

| NAV-3f | J=0.00272700±0.00000( Spectro : VG 3600 | | | | | | | | | | | | | | | |
|---|---|---|---|---|---|---|---|---|---|---|---|---|---|---|---|---|
| **Relative Abundances** | | 36Ar [V] | %1s | 37Ar [V] | %1s | 38Ar [V] | %1s | 39Ar [V] | %1s | 40Ar [V] | %1s | 40(r)/39(k) ± 2s | Age ± 2s (Ma) | 40Ar(r) (%) | 39Ar(k) (%) | K/Ca ± 2s |
| 33260_AR | 600 °C | 0.0000303 | 53.662 | 0.0003365 | 92.443 | 0.0000662 | 26.204 | 0.0008544 | 5.743 | 0.0137850 | 2.924 | 5.68804 ± 11.30657 | 27.83 ± 54.90 | 35.25 | 0.15 | 1 ± 2 |
| 33261_AR | 650 °C | 0.0000194 | 75.313 | 0.0004149 | 74.920 | 0.0001216 | 13.749 | 0.0038414 | 0.692 | 0.0686538 | 0.572 | 16.37933 ± 2.27331 | 79.02 ± 10.73 | 91.64 | 0.66 | 4 ± 6 |
| 33262_AR | 700 °C | 0.0000745 | 19.418 | 0.0000597 | 521.472 | 0.0001942 | 8.529 | 0.0083573 | 0.612 | 0.0925542 | 0.431 | 8.43301 ± 1.03260 | 41.11 ± 4.98 | 76.15 | 1.44 | 60 ± 628 |
| 33263_AR | 750 °C | 0.0003261 | 15.991 | 0.0000765 | 589.195 | 0.0003058 | 8.150 | 0.0156988 | 0.216 | 0.1257348 | 0.765 | 1.86222 ± 1.96744 | 9.16 ± 9.65 | 23.25 | 2.70 | 88 ± 1040 |
| 33264_AR | 800 °C | 0.0001342 | 38.761 | -0.0001787 | 252.192 | 0.0004710 | 5.334 | 0.0288385 | 0.219 | 0.0990994 | 0.956 | 2.05119 ± 1.06820 | 10.09 ± 5.24 | 59.69 | 4.95 | -69 ± 350 |
| 33265_AR | 850 °C | 0.0000968 | 53.933 | 0.0001908 | 236.068 | 0.0010055 | 3.966 | 0.0689251 | 0.184 | 0.1679506 | 0.563 | 2.01224 ± 0.44874 | 9.90 ± 2.20 | 82.58 | 11.84 | 155 ± 733 |
| 33266_AR | 900 °C | 0.0002073 | 10.139 | 0.0007232 | 42.946 | 0.0023209 | 1.764 | 0.1894340 | 0.207 | 0.3999653 | 0.176 | 1.77859 ± 0.06645 | 8.75 ± 0.33 | 84.24 | 32.53 | 113 ± 97 |
| 33267_AR | 950 °C | 0.0001615 | 4.771 | -0.0005931 | 35.101 | 0.0012941 | 1.698 | 0.1271947 | 0.164 | 0.2720278 | 0.281 | 1.75335 ± 0.03830 | 8.63 ± 0.19 | 81.98 | 21.84 | -92 ± 65 |
| 33268_AR | 1000 °C | 0.0000944 | 9.413 | 0.0002402 | 87.036 | 0.0008270 | 2.667 | 0.0582583 | 0.180 | 0.1295069 | 0.491 | 1.73497 ± 0.09302 | 8.54 ± 0.46 | 78.05 | 10.00 | 104 ± 182 |
| 33270_AR | 1450 °C | 0.0001905 | 27.384 | 0.0005923 | 76.000 | 0.0010664 | 2.254 | 0.0809093 | 0.187 | 0.2736496 | 0.432 | 2.67738 ± 0.38234 | 13.15 ± 1.87 | 79.16 | 13.89 | 59 ± 89 |
| | S | 0.0013351 | 8.254 | 0.0018623 | 60.878 | 0.0076728 | 1.084 | 0.5823119 | 0.087 | 1.6429275 | 0.150 | | | | | |

**TABLE DR3 (continued)**

| Step<br>NAV-4f<br>Spectro : VG 3600 | Temperatur<br>°C | 40Ar/39Ar | 38Ar/39Ar | 37Ar/39Ar | 36Ar/39Ar<br>(E-3) | 39Ar<br>(E-14)<br>moles | %39Ar<br>released | %40Ar* | 40Ar*/39K | Age<br>Ma | ± s.d. |
|---|---|---|---|---|---|---|---|---|---|---|---|
| J= 0.002727 | | | | | | | | | | | |
| 1 | 350 | 233329.16 | 1.04 | 66.39745 | 1039.77 | 0 | 0 | 99.87 | 0 | 0 | ± 0 |
| 2 | 450 | 477.918 | 0.409 | 0.01935 | 1647.584 | 0.015 | 3.91 | -1.88 | -8.96 | 0 | ± 0 |
| 3 | 550 | 8.185 | 0.118 | 0.0005 | 22.722 | 0.016 | 8.2 | 17.72 | 1.45 | 7.121 | ± 3.503 |
| 4 | 600 | 1644181.3 | 1.04 | 66.39745 | 5898367.2 | 0 | 8.2 | -6.01 | -103237.8 | 0 | ± 0 |
| 5 | 650 | 8.153 | 0 | 0.00269 | 77.269 | 0.003 | 9.01 | -180.3 | -14.7 | 0 | ± 0 |
| 6 | 700 | 6.563 | 0.021 | 0.00012 | 7.719 | 0.067 | 26.42 | 64.94 | 4.26 | 20.848 | ± 0.988 |
| 7 | 750 | 6.456 | 0.008 | 0.00016 | 7.304 | 0.052 | 40.09 | 66.26 | 4.28 | 20.923 | ± 1.073 |
| 8 | 800 | 10.924 | 0.015 | 0.00011 | 22.598 | 0.073 | 59.13 | 38.69 | 4.23 | 20.676 | ± 1.731 |
| 9 | 850 | 6.353 | 0.014 | 0.00011 | 0.002 | 0.075 | 78.77 | 99.68 | 6.33 | 30.89 | ± 0.089 |
| 10 | 900 | 8.322 | 0.012 | 0.00021 | 0.003 | 0.039 | 89.07 | 99.75 | 8.3 | 40.385 | ± 0.211 |
| 11 | 950 | 26.545 | 0.032 | 0.00157 | 24.211 | 0.005 | 90.45 | 72.97 | 19.37 | 92.865 | ± 18.47 |
| 12 | 1000 | 31.473 | 0 | 0.00246 | 18.469 | 0.003 | 91.33 | 82.6 | 26 | 123.561 | ± 8.969 |
| 13 | 1200 | 6.321 | 0.002 | 0.00038 | 8.767 | 0.022 | 97.05 | 58.7 | 3.71 | 18.162 | ± 2.383 |
| 14 | 1450 | 8.936 | 0 | 0.00073 | 25.99 | 0.011 | 100 | 13.83 | 1.24 | 6.07 | ± 6.384 |

| Step<br>CAU-3f<br>Spectro : VG 3600 | Temperatur<br>°C | 40Ar/39Ar | 38Ar/39Ar | 37Ar/39Ar | 36Ar/39Ar<br>(E-3) | 39Ar<br>(E-14)<br>moles | %39Ar<br>released | %40Ar* | 40Ar*/39K | Age<br>Ma | ± s.d. |
|---|---|---|---|---|---|---|---|---|---|---|---|
| J= 0.002727 | | | | | | | | | | | |
| 1 | 550 | 5.946 | 0.211 | 0.00042 | 27.703 | 0.019 | 4.68 | -38 | -2.26 | 0 | ± 0 |
| 2 | 600 | 4.964 | 0.071 | 0.00056 | 0.009 | 0.014 | 8.2 | 99.54 | 4.94 | 24.146 | ± 0.216 |
| 3 | 650 | 6.494 | 0.026 | 0.00027 | 3.348 | 0.029 | 15.57 | 84.46 | 5.49 | 26.786 | ± 1.404 |
| 4 | 700 | 6.145 | 0.021 | 0.00017 | 6.785 | 0.047 | 27.41 | 67.05 | 4.12 | 20.159 | ± 2.29 |
| 5 | 750 | 5.065 | 0.02 | 0.00008 | 3.36 | 0.097 | 52.01 | 80 | 4.05 | 19.826 | ± 1.234 |
| 6 | 800 | 9.738 | 0.021 | 0.00009 | 19.76 | 0.088 | 74.3 | 39.84 | 3.88 | 18.985 | ± 0.934 |
| 7 | 850 | 5.171 | 0.02 | 0.00013 | 2.684 | 0.061 | 89.72 | 84.27 | 4.36 | 21.315 | ± 0.494 |
| 8 | 950 | 11.343 | 0.048 | 0.00039 | 9.709 | 0.02 | 94.84 | 74.53 | 8.45 | 41.119 | ± 1.734 |
| 9 | 1000 | 28.501 | 0 | 0.00398 | 61.908 | 0.002 | 95.34 | 35.75 | 10.19 | 49.439 | ± 11.841 |
| 10 | 1200 | 13.136 | 0.009 | 0.53894 | 10.137 | 0.015 | 99.15 | 77.29 | 10.16 | 49.29 | ± 1.805 |
| 11 | 1450 | 52.209 | 0 | 30714.419 | 59.822 | 0.003 | 100 | 99.96 | -99.93 | 0 | ± 0 |

**TABLE DR3 (continued)**